V. BRAYTON CYCLE TECHNOLOGY

Warner L. Stewart, William J. Anderson, Daniel T. Bernatowicz,
Donald C. Guentert, Donald R. Packe, and Harold E. Rohlik

INTRODUCTION

The space power sources discussed in this conference can be divided into two general categories. The first, static sources, includes batteries, thermionic generators, solar cells, and fuel cells; it represents the direct-power conversion systems in which heat or chemical energy is converted directly into electrical current. The second, dynamic power sources, converts heat into electrical energy through an intermediate step that involves mechanical work. Power systems of this type include the familiar Rankine and Brayton systems and are of principal interest in the low kilowatt to megawatt level.

Although the Brayton cycle has been known for almost a century, the embodiment of its principles into practical engines occurred only in the last three decades through the development of the modern gas turbine engine. The principle by which this engine works is illustrated in figure V-1 where the major components required for airbreathing power applications are indicated. Air enters the compressor where its pressure is substantially raised. This high-pressure air then enters the combustor chamber, where fuel is added and burned. The high-pressure, high-temperature gas then expands through a turbine, spinning it, and producing mechanical work. Approximately two-thirds of this work is used to power the compressor, and the remaining one-third is used to drive the generator which, in turn, produces the useful electrical power.

When the Brayton cycle is applied to a space power system, the fundamental cycle as just described remains the same. However, since it is operating in a space environment, some modifications must be made. Such modifications can be noted in figure V-2 where the compressor, turbine, and generator previously described are shown in the lower right portion of the figure. The three major modifications include the following:

(1) Since there is no air in space, the loop must be closed to reuse and to conserve the working gas. This closed-loop operation actually represents a considerable advantage, since it permits the use of working fluids with properties much more desirable than air.

(2) Because of the closed-loop operation and the extended times of operation, the heat source must be of a different nature. Rather than burning fuel, heat sources such as solar and nuclear energy must be used. The heat so generated must then be transferred into the working loop by means of the indicated heat source exchanger.

(3) Provision must be made to reduce the temperature of the gas prior to redirecting it back to the compressor. This is done by first passing the exhaust gas through a heat exchanger called

a recuperator, where heat is transferred back into the working fluid at the compressor exit. Such a step has the additional advantage of preheating the gas prior to going into the heat source and, thus, it improves substantially the efficiency of the cycle. Final cooling then takes place in the heat sink heat exchanger, where the remaining waste heat is transferred to a heat rejection loop. The heat is piped through a radiator where it is finally rejected to space.

From these considerations, it is evident that, although the basic cycle remains the same, additional components and considerable complexity arise when such a system is applied to space use.

The interest in the Brayton cycle for space power occurs for many reasons: (1) the extensive technology gained during the last 30 years in the gas turbine field can be drawn on and applied, (2) it has excellent prospects for applications where extended operation is required, (3) it is versatile in that a given system can cover a range of power levels and can be applied to a broad range of heat sources, and (4) it has potentially high cycle efficiency, thus making it a strong candidate for low-power applications where heat sources such as isotopic and solar energy are used and input energy is at a premium.

This interest has stimulated an extensive technology program at the Lewis Research Center aimed at obtaining a better understanding of its potential and exploring special problems that arise in its application. This paper reviews the technology program in terms of objectives, scope, and progress. Three general areas are discussed: (a) a review of the Brayton features as applied to a space power system, (b) a component technology discussion involving the performance and mechanical integrity of both rotating and heat transfer components, and (c) a system technology discussion directed at the questions of system control and startup.

BRAYTON POWER SYSTEM FEATURES

CYCLE DESCRIPTION

A better understanding of the features of the Brayton power system can be obtained by a comparison with the vapor, or Rankine, system. To do this, it is convenient to look at the temperature-entropy diagrams for the two cycles shown in figure V-3. In the Rankine cycle, a pump is used to pump the condensate returning from the radiator from a pressure corresponding with the condensing temperature up to a pressure corresponding with the boiling temperature. The liquid at high pressure is heated to boiling temperature, boiled along a constant temperature line, and expanded down to condensing pressure and temperature in a turbine that drives a generator. The vapor is then condensed and returned to the pump. It is important to note that the pressures in this cycle are determined by the vapor pressure - temperature relation of the working fluid and are not independent of the temperatures.

In the Brayton cycle, a compression process is followed by heating at approximately constant pressure, first in the recuperator and finally in the heat source where the gas is heated to the turbine inlet temperature. The gas is expanded through the turbine and is then cooled along an essentially constant pressure path, first through the recuperator and then through the radiator where the waste heat is rejected. The cycle is completed as the cooled gas from the radiator is returned to the compressor. Because this is a gas cycle rather than a vapor cycle, the cycle pressure level is independent of the temperature.

In a comparison of the characteristics of the two cycles, it is first noted that the working fluids of interest in the Rankine cycle systems are liquid metals and involve a phase change. The working fluids in the Brayton cycle systems, on the other hand, are inert gases and involve no phase change. Certain problems or characteristics appear as a result of the nature of the working fluids involved in the two cycles.

The Rankine cycle, which utilizes a two-phase fluid, must contend with the problems of phase separation in a zero-g environment in both the boiling and condensing processes. The single-phase Brayton cycle is not subject to such zero-g effects. The liquid-metal working fluid of the Rankine cycle introduces problems associated with corrosion and mass transfer, while the use of an inert gas in the Brayton cycle eliminates such problems.

The two-phase Rankine cycle, however, offers a distinct advantage over the Brayton cycle in pump work, in that the pump work required to pump a liquid is much less than the compressor work required to compress the gas in the Brayton cycle. In a typical Brayton cycle system, almost two-thirds of the turbine work may be required to drive the compressor, leaving only one-third of the turbine work available as useful work. Because the useful work is rather small compared with the compressor or turbine work, a small percentage change in compressor or turbine work, resulting from small changes in efficiency or system pressure loss, will cause a relatively large percentage change in useful work. It can be seen, then, that the Brayton cycle performance is very sensitive to these factors, and there is a strong incentive to minimize system pressure losses and to maintain high turbomachinery efficiencies.

Another important difference between the Rankine and Brayton cycles is the cycle temperature ratio at which they operate. The cycle temperature ratio is defined as the ratio of the minimum temperature in the cycle, that is, the radiator discharge or compressor inlet temperature, to the maximum temperature in the cycle or the turbine inlet temperature. One minus this cycle temperature ratio is equal to the Carnot efficiency. As can be seen from the temperature-entropy diagram, the Rankine cycle operates at a much higher cycle temperature ratio than does the Brayton cycle. This is because of the pressure-temperature relation of a vapor in the Rankine cycle, such that low cycle temperature ratios are associated with very high expansion ratios, of the order of 100 to 1 at a cycle temperature ratio of 0.6. Thus, in Rankine systems of interest for space application, turbine problems associated with excessive expansion ratios and pump problems associated with low suction head place a lower practical limit on the cycle temperature ratio. The Brayton cycle, on the other hand, permits an independent selection of pressure and temperature, and the selection of turbine expansion ratio and cycle temperature ratio is reached through an optimization procedure involving tradeoffs between cycle efficiency and radiator area requirements. This procedure results typically in turbine expansion ratios around 2 to 1 or less and cycle temperature ratios around 0.25 to 0.30.

CYCLE EFFICIENCY

The capability of the Brayton cycle to operate at low cycle temperature ratios is favorable from the standpoint of cycle efficiency, as shown in figure V-4. In this figure, cycle efficiency is plotted as a function of cycle temperature ratio for both the Brayton and the Rankine cycles. The crosshatched area represents the region of minimum practical cycle temperature ratio for the Rankine cycle, as previously discussed. Both curves show increasing cycle efficiency with decreasing cycle temperature ratio, but it can be seen that the Brayton cycle operates at cycle temperature ratios around 0.25 to 0.3, while the Rankine cycle is constrained to operate at cycle temperature ratios of around 0.65 to 0.7 or above. As a result, Rankine cycle efficiencies are lower than Brayton cycle efficiencies, even though the Rankine cycle is thermodynamically a more efficient cycle when operating between the same temperatures, that is, at the same cycle temperature ratio.

RADIATOR AREA

Although low cycle temperature ratios are favorable from the standpoint of high cycle efficiency, the associated low radiating temperature results in large radiator areas. This effect is shown in figure V-5, where specific prime radiator area is plotted as a function of cycle temperature ratio for a Brayton cycle and a Rankine cycle operating at a turbine inlet temperature of 1950° R and a sink temperature of 400° R. The crosshatched area again represents the region of limiting cycle temperature ratio for the Rankine cycle. It is seen that the Brayton cycle radiator area is quite sensitive to cycle temperature ratio as compared with the Rankine cycle and is an order of magnitude higher.

Because of this large radiator area requirement, a Brayton cycle operating at current turbine inlet temperatures in the range of 2000° R is of primary interest in relatively low power applications, measured in tens of kilowatts, where radiator area is not so dominant and high cycle efficiency may be important. Solar- and isotope-powered systems are examples of low power systems, where high cycle efficiency is desirable from the standpoint of minimizing the required size of a solar concentrator in a solar system or minimizing the isotope inventory requirements of an isotope-powered system.

It would be possible to reduce significantly the radiator area requirement of the Brayton cycle if turbine inlet temperatures could be increased. This effect is shown in figure V-6 where minimum specific prime radiator area is plotted as a function of turbine inlet temperature in $^{\circ}$R for a sink temperature of 400° R. If the turbine inlet temperature could be increased to 3000° R, the specific radiator area could be reduced to one-third of that area required at present turbine inlet temperatures of about 2000° R. If material properties can be improved to a point where such increases in turbine inlet temperature can be achieved, the Brayton cycle may become of interest at higher power levels.

PRESSURE LEVEL AND MOLECULAR WEIGHT EFFECTS

It has been pointed out that the pressure level of the Brayton cycle can be selected independently of the cycle temperatures. Freedom to adjust pressure level is useful in two ways. First, it permits the use of the same turbomachinery over a range of power levels through changes in pressure level. For example, the power of the compressor and turbine can be doubled by doubling the pressure. In this way, one set of turbomachinery could be the heart of a variety of power systems. Second, it permits a choice of the size of the components for any particular power range. In particular, it permits the use of more nearly optimum-sized turbomachinery. At low power levels where mass flows are small, the pressure level can be reduced to keep volume flows at reasonable levels. In this manner, extremely small turbomachinery diameters for which it is difficult to maintain high efficiency can be avoided. At low pressure levels, however, a penalty is paid in the form of larger heat exchanger components.

Another important variable affecting turbomachinery geometry in terms of both number of stages and size is the gas molecular weight. Figure V-7 shows the number of turbomachinery stages required and the relative size or diameter as a function of molecular weight. The number of stages shown is for an application for which one stage is required with argon (mol. wt, 40), and the size is shown relative to that required with argon. As molecular weight is decreased, the number of turbine stages required increases rapidly. Thus, an application requiring a single turbine stage with argon (mol. wt, 40) would require 2 stages with neon (mol. wt, 20) and 10 stages with helium (mol. wt, 4). At higher molecular weights, less than 1 stage is shown to be required. For these higher molecular weights, a single stage would be used, but it could be operated at lower speeds and stresses with obvious benefits.

Figure V-7 shows that, as molecular weight is increased, the turbomachinery diameter increases. For low power machinery, this can be a helpful trend. For example, a compressor that would be only 3 inches in diameter if argon were used, would be 20 percent larger, or 3.6 inches in diameter, with krypton (mol. wt, 83).

Gases of high molecular weight, therefore, are favorable to the turbomachinery, but these benefits are not obtained without some penalty. Here, a penalty is paid in increased heat exchanger size. This effect is shown in figure V-8, in which the bars indicate relative heat exchanger size (volume) associated with each of five inert gases, helium, neon, argon, krypton, and xenon, with the size normalized to 1 at helium's molecular weight of 4. The heat exchanger size associated with each of the pure gases increases with increasing molecular weight. A heat exchanger designed for use in argon is about 6 times as large as one designed for use in helium to meet the same requirements, while one designed for use in xenon would be almost 15 times as large. It is apparent, then, that the choice of the working fluid involves a tradeoff between the turbomachinery and the heat exchanger components.

It is possible to achieve the benefits of high molecular weight from the standpoint of the turbomachinery without such a large sacrifice in heat exchanger size through the use of mixtures of these inert gases rather than the pure gases. As long as the molecular weight is the same, the mixture and the pure gas behave the same in the turbomachinery, and the previous discussion about number of stages and diameter applies as well to mixtures. However, the thermal conductivity can be substantially improved by mixing the highly conductive helium with a heavy gas, like xenon, to give the desired molecular weight. The curve labeled helium-xenon gas mixture shows that, for each intermediate molecular weight (neon, argon, krypton), the improved conductivity of the mixture reduces the heat exchanger size to almost half.

Current interest is in gases with molecular weights in the range of 40 to 80 for power levels from a few kilowatts to a few tens of kilowatts. In this range, the use of gas mixtures appears to be an attractive method for improving the heat transfer characteristics of the Brayton cycle working fluids, if problems such as possible preferential leakage of helium from the system are not encountered.

COMPONENT TECHNOLOGY

From the cycle discussion, it is evident that the components must have high performance in order to exploit the performance potential afforded by the Brayton cycle. In addition, these components must have within them the ingredients that give them high mechanical integrity and long life capability. These two concerns, performance and mechanical integrity of the components, are discussed herein. The section is divided into two major subareas, rotating components, which have more general application, and heat transfer components, some aspects of which must be tied to more specific applications.

ROTATING COMPONENTS

The discussion of the rotating components is divided into four parts. The first two deal with the performance aspect of the turbomachinery and generator involved, whereas the last two are concerned with the packages involved when these components are put together. The first of these sections discusses the use of gas bearings applied to Brayton packages, and the last part describes the results obtained to date in the investigation of one such package.

Turbomachinery Aerodynamics

Design considerations. - In the selection of turbomachinery for Brayton space power systems, two candidate compressors appear suitable, the single-stage centrifugal and the multistage axial. On the drive end of the shaft, radial- and axial-flow turbines may also be considered. The units shown in figures V-9 and V-10 are the rotors of two matched sets of turbine and compressor designed for a particular Brayton system. The compressor rotors (fig. V-9) includes a 6-inch-diameter radial-blade centrifugal unit and a six-stage 3.5-inch-diameter axial unit. The radial in-flow turbine rotor (fig. V-10) is about 6 inches in diameter and was designed to drive the centrifugal compressor. The axial turbine shown drives the six-stage compressor and has a tip diameter of 5.1 inches. The size of these components brings up several questions regarding fabrication and performance, and the importance of high component efficiency indicates careful consideration of the factors that influence efficiency. These have been explored in a program combining in-house and contract efforts.

There are several areas that must be considered before the turbine and compressor components of a given system are designed. Three major areas of concern include the selection of design point conditions consistent with high efficiency, the use of optimum geometry, and the influence of small size and low Reynolds number on performance.

The selection of the design point operating conditions involves the use of optimum velocity diagrams, and selection of an optimum velocity diagram involves the use of curves such as that shown in figure V-11. In figure V-11, turbine efficiency, based on total pressures at the inlet and outlet, is shown as a function of the ratio of turbine tip speed to the isentropic gas velocity corresponding to the turbine expansion process. This ratio is commonly used to identify turbine velocity diagrams and the shape of the curve is typical of both radial and axial turbines. Efficiency goes to zero at zero speed and also at a high speed where the blades overspeed the gas flow to the extent that no turning takes place in the rotor.

The data points on the curve were obtained with the 6-inch radial turbine. The peak efficiency of 0.88 is quite satisfactory for this application and compares favorably with much larger turbines. The occurrence of peak efficiency at a velocity ratio of 0.7 is consistent with previous work in radial inflow turbines.

After selection of the optimum velocity diagram, the influence of overall geometry must be considered. Figure V-12 shows how geometry considerations affected the selection of rotative speed for the 6-inch radial turbocompressor. In figure V-12, compressor efficiency and tip radius are shown to vary with shaft speed for a given set of gas conditions and flows. The cross sections are compressor impellers corresponding to various combinations of radius and shaft speed when tip speed is fixed by the required pressure ratio and velocity diagram considerations. The inlet is about the same in each cross section. This results from an essentially constant volume flow as governed by cycle conditions. The impeller shape is, therefore, a function of speed. Past experience in the field has produced the illustrated efficiency variation, showing, for this example, an optimum speed near 35 000 rpm. The cross section here, then, shows the optimum overall geometry. The speed range shown in figure V-12 (35 000 to 60 000 rpm) includes the speeds of interest in Brayton space power systems.

Another consideration in the selection of the design point is associated specifically with the compressor. This may be seen in figure V-13, which shows experimental performance in argon of the 6-inch centrifugal compressor. Pressure ratio is plotted as a function of weight flow, ratioed to the design flow, for lines of constant speed. Efficiency is shown as contours superimposed on the speed lines. The location of the design point shows that the design combination of pressure ratio, speed, and flow was achieved in this design. The operational boundary on the left is the compressor surge line, which represents a condition of violent flow fluctuations with induced shaft and blade vibrations. Figure V-13 shows that the maximum efficiency at each speed occurs near the surge line. Safe operation of the compressor, however, requires a margin between surge and the design point. This involves a sacrifice in efficiency of about 2 points.

The selection of design point velocity diagrams, therefore, is made on the basis of an optimum blade-to-gas velocity ratio which yields maximum efficiency. Optimum geometry, also corresponding to maximum efficiency, is the influencing factor in the selection of rotating speed. In addition, to ensure safe operation of the compressor, there must be a safe margin between surge and any programed operation.

Reynolds number and size effects. - The effect of Reynolds number on boundary layer behavior has been studied rather extensively. As Reynolds number is reduced in the turbulent regime, a progressive thickening of the boundary layer occurs. As Reynolds number is reduced further, the flow in the boundary layer becomes laminar, and separation and increased loss are likely to occur. In order to determine the extent to which Reynolds number influences performance, experimental investigations were made over a wide range of Reynolds number using the 6-inch radial turbine and the 6-inch centrifugal compressor. Results of these tests are shown in figure V-14, in which total efficiency is plotted against Reynolds number based on rotor blade chord. Although a wide range in Reynolds number was covered, no sharp decreases in efficiency were observed. This indicates that there were no pronounced effects of laminar flow separation. The design Reynolds number for the compressor is about 300 000, and the maximum experimental efficiency was 0.79 at design speed.

The turbine efficiency was 0.88 at design speed, pressure ratio, and Reynolds number. The drop in efficiency, therefore, was only 0.02 in decreasing Reynolds number from 150 000 to the design value. The difference in efficiency levels between the compressor and turbine reflects the fact that turbines benefit from the accelerating internal flow, while the compressor must cope with appreciable flow decelerations and consequent higher losses. It can be pointed out that there is some concern regarding the performance of the axial flow machinery. The very short blade chords in both turbine and compressor result in design Reynolds numbers of 20 000 and 75 000, respectively. These axial flow machines are now being tested to determine the extent to which these low Reynolds numbers influence the efficiency levels.

Reynolds number and size are related directly by the characteristic length in the Reynolds number equation. There are other considerations, however, that obscure this relation when Reynolds number loss correlations are attempted. Other size factors include contour coordinate accuracy, flow area control, running blade tip clearances, and surface roughness. Therefore, a size study was initiated in the Lewis technology program. Figure V-15 shows the impeller of the 6-inch centrifugal compressor described previously and a similar compressor 3.2 inches in diameter. The tip diameter ratio is almost 2 to 1, and the flow area ratio is about 3.5 to 1. Also, a radial inflow turbine was made geometrically similar to that described in the Turbomachinery Aerodynamics section. The two rotors are shown in figure V-16. The tip diameters are 6.0 and 4.6 inches and result in a diameter ratio of 1.3 and an area ratio of 1.7. These machines were tested over a range of Reynolds number, and the efficiencies are shown in figure V-17. Turbine total efficiencies plotted were measured at design equivalent speed and pressure ratio and, consequently, at the design value of blade-to-ideal-gas velocity ratio. The compressor efficiencies, however, are the maximum values of efficiency at design equivalent speed. Earlier correlations using design flow or pressure ratio at design speed were questionable because of the effects of thickened boundary layers on flow and also impeller-diffuser mismatch as Reynolds number was reduced. Both the compressor and the turbine show some size and Reynolds number effects. The differences associated with size vary from only a point or so in the compressor to two or three points in the turbine. From this, it can be concluded that size and Reynolds number can be important in space power system components, so some care must be exercised in selecting these parameters. The efficiency levels being achieved, however, are satisfactory for low-power Brayton applications.

Electric Generator

The electric generator converts the available shaft power into electric power to supply the many and varied loads that are typical of space power systems. In order to be applicable for a space power Brayton system, a generator must meet the following two criteria: it must be very reliable in order to operate over extended periods of time with zero maintenance, and it must convert mechanical to electrical power with high efficiency. In general, all other factors such as weight and size are of secondary importance in this application.

Reliability. - The question of reliability will be considered by first reviewing the conventional alternating current generator or alternator concept. Figure V-18 shows a simplified diagram of a conventional two-pole alternator with the field winding on the rotor. This machine has both brushes and slip rings on the shaft to carry current through the rotating field windings. The brushes are a continuous point of friction and wear and a source of contaminant particles for a space power system and are, therefore, a potential cause for unreliable operation. Because of the stringent reliability requirement, the brush slip ring concept is considered unsuitable for space power applications. While it is true that brushes can be eliminated by an additional winding and rotating rectifiers, as is popular in the aircraft industry, it is desired to improve further the inherent reliability of a space power system alternator by removing the windings entirely from the rotor, leaving only a solid magnetic path.

In an alternator, voltage is generated by the time rate of change of flux through the armature windings. Thus, any arrangement that causes flux variation with rotation will induce voltage in an armature coil. One such arrangement is shown in concept in figure V-19. This machine has both field and armature windings on the stator, the stationary magnetic element. The rotor has no windings. As the shaft rotates, once each revolution, the rotor pole faces become alined with the stationary pole faces and, at this point, maximum flux through the iron occurs; at 180° rotation from this maximum, a minimum flux condition occurs. The changing flux thus induces armature voltage. Also, the flux through the rotor is always unidirectional because of the axial offset of the pole faces. In a real machine of this type with a cylindrical stator, the flux is not only unidirectional but constant as well. This constancy of flux all but eliminates eddy current heating losses in the rotor iron and, except for the pole faces, permits solid rather than laminated construction. One additional advantage of the solid rotor is that the field losses, which result in heat, occur on the stator in this type of machine, where cooling can be more easily provided.

Therefore, even though the conventional wound rotor alternator is lightweight and more efficient, the overriding reliability requirement indicates that the solid rotor alternator has the best potential for space power application.

There are many variations of solid rotor alternators. The choice of which variation to use depends on the system requirements. In the Turbomachinery Aerodynamics section, it is pointed out that, in order to achieve good performance, the turbocompressor shaft speed must run typically between 30 000 and 60 000 rpm. Solid rotor alternators, on the other hand, are better suited to a lower speed range, typically 10 000 to 40 000 rpm. In addition, the lower speeds are more desirable on the basis that power at 400 cps, which is a standard aircraft frequency for which there exists a vast technology and a wide variety of off-the-shelf devices, can be generated directly only at the lower speeds, for example at 12 000 rpm in a four-pole alternator. Depending therefore on the requirements, the configuration of the Brayton system may be either a one-shaft or a two-shaft system, as shown in figure V-20.

The single-shaft system, shown in figure V-20(a), combines the turbine, alternator, and compressor on the same high-speed shaft, while the two-shaft system (fig. V-20(b)) has only the compressor and its turbine on a high-speed shaft and the alternator with a second turbine on a low-speed shaft. The single-shaft system has the advantage of being compact in size and easily integrated into the system. The two-shaft system is somewhat larger in total size and more difficult to integrate into the system; however, it provides lower output-power shaft speeds and allows independent development of both rotating packages.

Efficiency. - Efficiency is, of course, influenced by many factors. For the high speed alternators, windage losses are a significant element of efficiency. Thus, for high-speed operation, it would be desirable to design a rotor with a smooth surface. Figure V-21 shows a two-pole alternator rotor of this type. The bottom view shows the two-pole pieces before assembly. In the assembled rotor shown at the top, magnetic pole piece separation has been achieved by the use of a nonmagnetic filler material, in this case, Inconel. As can be seen, the rotor surface is smooth, which tends to minimize windage losses in the machine at high speed.

Where the system requirements permit a lower speed alternator configuration, a machine of the type shown in figure V-22 may be used. In figure V-22 is a view of the dissassembled alternator. In this machine, pole separation is achieved on the rotor both by axial displacement and by elevation of the pole faces. Windage losses are minimized by end plates. It may be noted that this is a four-pole alternator, as opposed to the two-pole conceptual machine shown in figure V-18. The use of four-pole construction on the rotor permits mechanical balancing, but it also has the effect of doubling the output frequency for the same shaft speed. This machine is rated at 12 kilowatt output at a speed of 12 000 rpm and a frequency of 400 cps.

As part of the Lewis Research Center program to investigate their performance, two solid rotor alternators have been built. Both are 12 000 rpm, 400 cps machines of similar design. They include the aforementioned Brayton system 12-kilowatt machine and a 60-kilowatt machine for the SNAP-8 Rankine system. Figure V-23 plots the performance of these two machines at a power factor of 0.8. The solid line is a curve generated from loss measurements made on the 12-kilowatt Brayton machine. The data points are measured efficiencies of the 60-kilowatt SNAP-8 machine. It can be seen that the efficiency of both machines is essentially flat at about 91 to 92 percent over a wide power range. These efficiencies are electromagnetic efficiencies and do not include bearing losses.

Tests to date show that the lower speed solid rotor alternators have satisfactory performance and, although the performance of the high-speed machines has not been demonstrated, no significant problems are anticipated.

Magnetic unbalance. - Magnetic unbalance is of concern in a Brayton alternator because of the use of gas bearings. Figure V-24 is a schematic view of one end of the rotor shaft. The problem in this machine arises from the fact that the two diametrically opposite pole faces are of the same magnetic polarity. When the rotor is centered, as in figure V-24(a), the flux is uniform on both pole faces and balance is achieved. If the centerline of the rotor is displaced as shown in figure V-24(b), however, the flux through the small gap will increase while the flux through the large gap will decrease, thereby creating a net force of attraction toward the smaller gap. As an example of the magnitude of the problem, analytical studies have shown that for the 12 kilowatt Brayton machine, a periodic force of attraction of up to 20 pounds would result from a 0.002-inch displacement in a machine with a 0.040-inch radial gap. The bearings would be required to supply an opposing force of equal magnitude. Studies, both analytical and experimental, are underway to fully evaluate this problem.

Gas Bearings

Design considerations. - Some of the system characteristics and operating conditions have a profound influence on bearing selection and design. (1) The system is required to operate for several thousand hours with a high degree of reliability and, during this time period, the inert gas working fluid must be kept clean. This makes it advantageous to use gas bearings. The use of oil-lubricated rolling bearings would result in greater power loss, weight, and complexity because of the need for seals and oil scavenge and separation systems. (2) The low pressure level and pressure ratio of the system dictate the use of self-acting or hydrodynamic bearings, which generate their own load capacity, as opposed to externally pressurized or hydrostatic bearings. Because of the low pressure drop available, purely hydrostatic bearings would not have sufficient load capacity unless the bearings were made quite large. (3) It is necessary for the power system to operate at high speeds and low loads to zero loads in a zero-gravity environment. This combination of operating conditions makes the stability characteristics of the bearings extremely important. Stable operation of the rotor or shaft in the bearing implies the absence of any motion of the shaft axis relative to the bearings other than simple synchronous eccentricity caused by shaft unbalance.

Journal bearings. - A conventional circular journal bearing, such as illustrated in figure V-25, is not suited for high-speed, low-load operation because of its tendency to be unstable. Under the action of a load, the journal center O_J deflects to form a fluid pressure wedge, but it does not move in the direction of the load. The resulting fluid film pressure force can therefore exert a moment about the bearing center O_B so that, if a momentary imbalance of forces occurs, it can drive the journal center into an orbital motion around the bearing center. This so-called whirl can destroy the bearing if its amplitude becomes great enough to cause a rub.

The most effective type of gas journal bearing in resisting whirl instabilities is the tilting or pivoted pad bearing. A four-pad pivoted journal bearing is shown in figure V-26. It consists of a journal and four pads, each of which is free to pivot so that it can adjust itself to the position of the shaft. Under zero external load conditions, a pivoted pad bearing can be set up geometrically so that each pad applies restoring forces to keep the shaft centered in the bearing. A wedge-shaped film is formed between each pad and the shaft, similar to that of a highly loaded ordinary journal bearing.

In addition to stability, load capacity, power loss, and running clearance are also important. The performance characteristics of a single pad of a typical three-pad bearing used in a Brayton turbocompressor are illustrated in figure V-27. Pad load capacity in pounds and pad friction in watts are shown as functions of minimum film thickness. The operating minimum film thickness is of the order of 0.0004 inch. At this minimum film thickness, the power loss is about 20 watts for one pad, or 60 watts for a three-pad bearing. This is reasonable but, in small machines of only a few kilowatts, output bearing power loss can be a problem, so care must be taken to maintain adequate film thickness.

A problem that must be considered with self-acting bearings is that they have no load capacity at startup when there is no relative motion of the surfaces. Therefore, to avoid surface contact at startup, which could result in damage to the critical bearing surfaces, a system of external pressurization is used. The arrangement used, shown in figure V-28, consists of a bearing pad mounted on a diaphragm with a ball and socket pivot. Pressurized gas is fed through the pivot to avoid attaching lines to the pad; attachments would increase pad restraint, which is detrimental to bearing stability. The fitted ball and socket pivot is used to minimize leakage of the pressurizing gas. Pressurized gas is fed to four orifices on the pad surface. Figure V-29 shows the three journal bearing pads. The four orifices for hydrostatic jacking can be seen in each of two pads, and the pivot socket can be seen on the back side of the third pad.

Thermal considerations. - As might be surmised from the small film thicknesses, the gas journal bearings are quite sensitive to thermal distortion and differential thermal growth of the shaft and pad carriers. Minimum film thickness must be maintained within rigid limits, as can be seen in figure V-30. The permissible limits of minimum thickness are shown in the area bounded by the crosshatching. The minimum film thickness at the operating point is of the order of 0.0004 inch. With the pad pivots rigidly mounted, it would require a differential temperature of only a few degrees Fahrenheit to either completely take up all the bearing clearance and get into the overload area shown on the left or to increase the bearing clearance and get into the unstable operation area shown on the right. In a hot machine, this is obviously unacceptable.

One way to overcome these problems of maintaining pivot film thickness within rigid limits in a hot machine in which the parts undergo drastic changes in temperature is by mounting one or more of the pads on a soft spring, such as the diaphragm shown in figure V-28. This makes the journal bearings quite tolerant to otherwise hazardous thermal conditions. The effect of pad mount stiffness on thermal tolerance is shown in figure V-31. The relative thermal growth that can be tolerated is shown in the area bounded by the crosshatching. With rigid pad mounts, only a small amount of relative thermal growth can be permitted, since all of it appears as a change in the film thickness. With a spring mount, however, a large relative thermal growth can be permitted, since very little of it appears as a change in film thickness. Practically all of it is taken up as a deflection in the spring mount. A soft spring mount thus makes the bearing very tolerant to thermal conditions.

Thrust bearings. - Two types of thrust bearings being considered for application in Brayton machinery are illustrated in figure V-32: these are the Rayleigh step bearing and the spiral groove bearing. The Rayleigh step bearing is composed of a number of segments (the bearing shown in fig. V-32(a) has eight), each with a feed groove, a step, and a land area. Clockwise rotation of the smooth-faced mating runner drags gas across each of the eight steps where it is compressed. Four jacking orifices, used for external pressurization at startup, are located on the lands of alternate sectors.

The spiral groove bearing utilizes a large number of very shallow spirally cut grooves. Counterclockwise rotation of a smooth-faced runner causes gas to be pumped radially inward. A pressure rise is created, which supports the load. In the spiral groove bearing, the jacking orifices are placed on the land area inside the grooves.

A photograph of the hydrodynamic thrust bearing used in a Brayton turbocompressor is shown in figure V-33. It is an eight-sector step bearing. The feed grooves, steps, and lands, as well as the four jacking gas orifices are visible in the figure.

Operating experience. - The operating experience to date with the Brayton turbocompressor at turbine inlet temperatures to 1250° F indicates that the bearings operate stably. Pains have been taken, however, to control the bearing thermal environment carefully. The magnetic loads imposed on the bearings in the turboalternator are still an unknown factor since this unit has not been operated. More work is required to develop bearings that are less thermally sensitive and generally more rugged.

In other machines such as helium blowers, gas bearings have demonstrated several thousand hours of reliable operation, although at lower temperatures than those in Brayton machinery.

Packaging

Temperature control. - The bearing considerations already discussed lead to numerous packaging problems, which include thermal isolation of the hot turbine area, minimum temperatures and temperature gradients in the bearing area, and flexibility in the bearing mounts. In order to explore and solve these problems, the turbocompressor component of a twin-shaft system is being operated at Lewis Research Center. This unit is shown in figure V-34. Visible are the compressor volute on the left, the turbine inlet scroll on the right, and the shell housing the bearing cavity between the two. The turbine and compressor are the radial units previously discussed. The package interior is shown schematically in figure V-35. Here again, the compressor is shown on the left and the turbine on the right. The thrust bearing, with a gimbaled stator, is mounted between the two journal bearings. The journal bearing cross section shows the low-spring-rate diaphragm mount of one pad in each journal bearing array of three pads. Three struts or columns, as shown at the bottom of figure V-35, support the compressor and turbine housings and the bearing carriers and thus control all running clearances.

Thermal isolation of the turbine area was accomplished with three major heat barriers; these include the thin-wall hollow section in the shaft adjacent to the turbine rotor, the two coated radiation shields, and the thin-wall hollow sections in each column at the hot end. These heat barriers interrupt the major heat paths as much as possible without sacrificing structural integrity.

Steps were also taken to minimize temperature gradients in the bearing area. Copper inserts in the shaft and column serve this purpose. The heat that does get through the heat barriers and the heat generated by bearing friction are removed by a small quantity of cooling gas and conduction to the compressor end of the package.

Preliminary investigation of the operating characteristics of the package has been made in a test facility that permitted slow starts and fine control of speed and flow. Figure V-36 shows the test installation with the shaft vertical in order to prevent gravity loads on the journal bearings. The compressor is at the top. About 70 instrument leads connect internal instruments with display and recording equipment in the control room. The investigation was made with turbine inlet temperatures up to 1000° F, and successful self-acting operation of the bearings was obtained. Measured temperatures in all bearing parts showed a range of 27° with an average of about 300° F. These tests indicate that temperature controls designed into the unit have been fairly effective. The level of all internal temperatures will increase, of course, as turbine inlet temperature is increased to the design value of 1500° F.

Critical speed and shaft vibration. - An important factor in the design and operation of any rotating machinery is critical speed. Care must be taken to ensure that none of the natural frequencies of the system coincide with or are even near the design speed. The first two critical speeds are the rigid body criticals; one involves a conical motion of the shaft while the other is a cylindrical motion. These frequencies depend to a large extent on the spring rates of the bearing mounts. A third critical speed involves shaft bending, and the speed at which it occurs depends largely on shaft stiffness. The radial turbocompressor was designed to have the first two criticals occur at very low speeds and the third well above the design speed. A rotating mass cannot be perfectly balanced; consequently, there will be some exciting force at the critical speeds that will result in rotating loads and shaft excursions within the bearings.

Since it is important to know both the location of critical speeds and the magnitude of shaft excursions, shaft displacement probes were mounted near each journal bearing. Figure V-37 shows the arrangement of the probes relative to the hard- and soft-mounted pads. The probes are located in radial planes just outboard of the bearing pads, and the two at each journal are spaced 90° apart so that their outputs can be fed into the x-y inputs of an oscilloscope to provide an image of shaft motion. Figure V-38 shows a group of shaft orbits as observed during a recent test run. Speed is shown in the upper right corner of each frame in hundreds of rpm. Figure V-38(a) shows stable rotation with little or no eccentricity. Figure V-38(b) shows an elliptical orbit with a major axis of 0.001 inch. This was observed as the shaft accelerated through one of the critical speeds. Figure V-38(c) is a near-circular orbit indicating simple eccentricity with a diameter of 0.0005 inch.

The taped record of an acceleration was used to prepare a plot of the shaft motion as a function of speed. Figure V-39 shows maximum shaft center displacement plotted against rotative speed. Five distinct peaks were measured with two of these corresponding to the first and second critical speeds calculated with the high spring rate of the gas film in series with the hard mount. Two additional peaks at lower speeds may be attributed to the low spring rate of the diaphragm mount and gas film. There are, therefore, four distinct rigid body criticals corresponding to the translatory and conical modes with the hard- and soft-mount spring rates. The reason for the fifth peak is not clear, but it appears to be a test rig resonance. There is very little shaft displacement as the rotative speed increased from about 16 000 rpm to the design speed of 38 500 rpm. The third or bending critical occurs at 56 000 rpm, well above the design speed.

The main observations made to date are that the first and second criticals occur well below the design speed and that the very small shaft displacement obtained near design speed should not cause any trouble in sustained design operation. High-temperature and long-term operations have not yet been attempted. During all operations to date, however, the bearings have operated satisfactorily and, on one occasion, a valve malfunction caused a rapid deceleration from 80 percent speed to zero through the compressor surge region of operation. The bearings, pressurized at the time, maintained running clearances and suffered no apparent damage.

HEAT TRANSFER COMPONENTS

The discussion of the Brayton components associated with the transfer of heat is divided into two parts. The first part will discuss the recuperator and heat rejection system whereas the second part will cover the heat source component. The three sources discussed include solar, radioisotope, and nuclear reactor.

Recuperator and Heat Rejection

It has been mentioned that, for the Brayton cycle, a recuperator with high effectiveness and low pressure drop is needed. Fortunately, the technology in heat exchangers is far enough advanced that such high performance heat exchangers are not a special problem. Presently a recuperator is being fabricated for use with argon and designed to give an effectiveness of 90 percent and a pressure drop of about 2 percent. The core geometry is of the counterflow, plate-fin type, and the core performance has been validated by tests on air.

The heat rejection subsystem shown in figure V-2 consists of a liquid loop coupled to the gas loop by a heat exchanger. Cooling the gas in the radiator, without a liquid loop, was also considered. It was found that the extra gas pressure drop would cause a drop in output greater than the power needed to pump the liquid, and that the gas radiator would be heavier despite the elimination of the temperature drop in the heat exchanger.

Also, any changes in the gas radiator would tend to change the gas pressure drop and directly affect system output, thereby making conversion system performance quite dependent on radiator location and configuration. With the liquid loop, however, the radiator shape and location could be changed to meet different vehicle integration constraints without affecting conversion system performance.

The only apparent disadvantage of the liquid loop is that it adds complexity to the system and would tend to reduce reliability. Generally, however, a liquid cooling loop is needed to cool other components, such as the alternator and electric components, and adoption of a liquid loop for the main heat rejection system means only an enlargement of the loop rather than an incorporation of additional components.

Therefore, it appears to be preferable to use the liquid loop rather than the gas radiator.

Heat Sources

The Brayton cycle can be used with any energy source that can provide heat at the proper temperature. For space applications, the energy sources of principal interest are the Sun, radioisotopes, and nuclear reactors. Each has its advantages and disadvantages, and these factors vary in importance with the application. The nuclear sources are compact and require no special orientation, but they are hazardous. The solar heat sources do not have the hazards that the nuclear ones do and require less technology advancement to make a usable system. However, they require orientation, special means to operate during shadow periods, and large areas to intercept the solar flux.

Solar heat source. - Figure V-40 shows a conceptual picture of a solar Brayton cycle system. The large concentrator or mirror focuses the sunlight into a receiver, in which the energy is transferred to the cycle gas. The conversion equipment is clustered around the receiver. The large, squat cylinder is the radiator and, in this concept, the concentrator could be stowed within it during launch.

To provide heat to a Brayton cycle furnishing 5 to 10 kilowatts of power, a concentrator 20 to 30 feet in diameter is required. In order to heat the cycle gas to 2000° R, the mirror surface accuracy required for high collection efficiency is moderate. To explore the problems of building a concentrator for the Brayton cycle, a prototype 20-foot-diameter unit is now being made. The approach in this program was to use conventional manufacturing techniques as much as possible and to avoid leaving residual stresses in the material to minimize changes in shape that might occur because of relief of stresses with time.

The concentrator consists of 12 magnesium sectors bolted together. A sector is seen at one step of the processing in figure V-41. The process is as follows: 1-inch-thick flat magnesium plates are polished on one side. Pockets are then machined into the back, leaving a ribbed structure that provides stiffening. These flat, machined sectors are placed on an accurately machined aluminum form, as in figure V-41. The form and sector are then heated and the load is applied to the sector, first mechanically by clamps (some of which are shown in fig. 41) and then by vacuum ports in the form. The sector is held at about 550° F under load for about 1 hour, and it deforms plastically and takes the shape of the form. The edges are machined to final dimensions and bolt holes are drilled.

An assembly is shown in figures V-42 and V-43, in which can be seen the ribbed back side and polished front. The polished magnesium surface is smooth but not shiny. The sectors are now being coated to make them mirrorlike. An epoxy layer is applied to the magnesium to give a glasslike surface on which the actual reflecting surface of aluminum is vacuum deposited.

The weight of this prototype is 1 pound per square foot. The geometric accuracy of this concentrator has not been fully evaluated yet, but preliminary measurements are encouraging.

The other solar heat source component is the receiver, which captures the concentrated solar energy and transfers it to the cycle gas. To provide the capability for power generation in the dark, some of the captured energy is stored in the receiver. The storage and release of this energy are accomplished by melting and freezing a material with a high heat of fusion, such as lithium fluoride.

Several different requirements must be met in the design of a receiver if it is to perform all its functions satisfactorily. The heat transfer into the cycle gas, the solar input, and the stored heat must be properly matched with respect to time as well as location. This can be accomplished only if the distribution of the fluoride is properly controlled. The distribution must be controlled in such a fashion that it is the same in zero g (for the ultimate use) and in 1 g (for meaningful ground testing). This distribution problem is difficult and crucial because lithium fluoride contracts 24 percent when it freezes. Therefore, the receiver must be designed to accommodate this contraction and expansion of fluoride. It is important to control the location of the fluoride, not only to provide the proper distribution of the stored heat but also to avoid the danger of rupturing the container when the fluoride melts and expands. The receiver must also be able to tolerate the repeated temperature transients and accompanying thermal stresses as it passes through the many Sun-shade cycles.

A program to build a receiver using the concept shown in figure V-44 is now in its early phases. The gas enters the header at the bottom, is heated as it passes through the array of tubes, and exits at the top. The solar energy enters through the aperture and shines on the tubes.

A cutaway of a portion of one of the tubes is shown in figure V-45. The gas passes through the central tube, and rosette fins inside the tube improve the heat transfer to the gas. A bellows-type tube surrounds the gas tube, and the fluoride is contained within it. Clearance is provided between the bottom of each convolution and the central tube. The type of freezing pattern expected is also shown. The contours indicate the freeze line at different times. When the fluoride is completely melted, it fills the bellows. When the receiver enters the shade period, the gas will cool the fluoride. The first freezing will occur on the surface of the inner tube, and the solid will form a seal at the bottom of each convolution. Freezing will then progress in sealed compartments and, when fully frozen, each compartment will have a void. Without the sealing, liquid from one compartment could flow into voids in other compartments and overfill them. On melting, the overfilled compartment would rupture. It is hoped that this compartmentalizing will control the fluoride distribution, and the bellows geometry will ease thermal stresses and provide a finning effect to reduce hot spots. Work is now being initiated to evaluate this concept.

Radioisotope heat source. - Figure V-46 shows a possible future space station with a radioisotope Brayton cycle power supply. The radioisotope fuel is located in the two small rectangles at the far end of the vehicle. Two Brayton conversion units behind them furnish a total of 13 kilowatts. The radiator is in the vehicle skin. The system is very compact and requires no special orientation.

It was pointed out in Paper IV that the availability of attractive isotopes is limited. Therefore, the Brayton cycle with its high efficiency is attracting considerable attention for use with radioisotopes. Power outputs up to 10 or 15 kilowatts can be foreseen for radioisotope Brayton systems.

The present effort on radioisotope heat sources for use with a Brayton cycle consists primarily of studies. A fully acceptable design has not yet been evolved, but the effort is progressing in that direction. Figure V-47 schematically illustrates the basic elements that are felt to be required in a radioisotope Brayton system. The heat source contains the radioisotope fuel and radiates heat to a heat exchanger in the conversion system. This heat exchange by radiation allows independent handling, replacement, and disposal of the heat source.

A shield protects the crew or payload. One of the principal problems is that of hazard, not only prior and during actual use, but even after use; that is, how is the spent heat source to be disposed of ? The best means of disposal appears now to be intact reentry from orbit and recovery on Earth. A reentry body for disposal is shown attached to the heat source (fig. V-47).

A door is shown as a means of cooling the fuel block by radiation in the event the conversion system fails and no longer draws heat. Such auxiliary means of cooling will also be necessary for shorter lived isotopes, which release excess power early in life. Heat sink material that may be needed to prevent melting of the heat source in certain accidents such as a fire on the launch pad is also shown in figure V-47.

These then are the basic elements that now appear to be required, and studies are continuing to define these elements more fully.

Reactor heat source. - Figure V-48 shows a possible configuration for a 150-kilowatt nuclear reactor Brayton system. The reactor, shield, radiator, and redundant Brayton conversion equipment including the turbomachinery, recuperator, and waste heat exchanger are shown. In this concept, the reactor coolant is a liquid metal, and a liquid-metal-to-gas heat exchanger is buried in the shield.

All reactor systems require a heavy shield, which is relatively independent of power level. Therefore reactor systems are not of interest for powers below 20 or 30 kilowatts. As power level increases, the reactor systems become more and more attractive and, at 100 kilowatts or more, reactor power systems are the leading candidates.

It will be recalled, however, that the Brayton cycle requires a large radiator (typically several times larger than a Rankine cycle). At the higher powers, integration of the Brayton radiator into the launch vehicle envelope becomes a serious problem. Therefore, there is more incentive with the reactor Brayton system to raise the turbine inlet temperature as high as possible, up to the limit set by reactor technology.

The leading concern at this time is the definition of the reactor for a Brayton cycle system. Several important questions must be resolved: should the reactor coolant be gas or liquid-metal? What is a practical target for reactor operating temperature? What fuel and cladding materials should be used? More study is required before the picture can be clarified and the best reactor Brayton system defined.

SYSTEM TECHNOLOGY

In a complex system such as the Brayton space power generating system, certain problems arise due simply to the assemblage of a large amount of equipment into an integrated, coordinated, functioning machine. These problems cannot be identified exclusively with any one component but rather with the interactions among the components of the system. Thus, there is indeed a technology associated with an assemblage of components, which is known as system technology.

System technology seeks to understand the important variables in system operation so as to configure and control the system to an optimum performance. Of particular concern in system technology are the establishment and maintenance of a suitable system operating point, safe and reliable start and shutdown procedures, control of critical operating variables such as alternator frequency, and the identification and specifications for all peripheral hardware components necessary to perform these tasks.

Three areas of system technology for Brayton systems are discussed herein, namely, alternator speed control, system power level control, and system start. This section is an attempt to give the reader an insight into system technology and therefore does not cover all the problems that may arise. It is intended, however, to be descriptive in significant system technology study areas.

ALTERNATOR SPEED CONTROL

Fundamentally, the speed is controlled by balancing the turbine and alternator torques at the design speed. Practically, however, the electrical load on the alternator may not be constant and may switch, for example, as much as full on to full off and back at any time. In order to achieve a continuous torque balance at design speed, one of two choices must be made, as illustrated in figure V-49. As shown in the top portion of the figure, speed control may be achieved by controlling the total alternator load to balance at all times the power input to the turbine. For this type of control, alternator output power, which is not consumed as useful load, is diverted to a parasitic load and dumped overboard. In the lower portion of the figure, speed is controlled by varying the input power to the turbine in correspondence with the electrical power consumption by the useful load. In this method, high performance valving can be employed to control turbine input power on an instantaneous basis, thus diverting transient excess power away from the turbine, while a secondary control can adjust the average primary heat source power level on a long term basis to conserve energy. For reliability, the alternator load method is preferable since it has no moving parts and can be built from very reliable solid-state electronic or magnetic elements. It can be seen, however, that unused power from the alternator is wasted. This wasted power is of no consequence if the primary heat source is either infinite energy, such as a solar source, or continual decay, such as an isotope heated source. If, however, the energy source is finite and conservable (e.g., a nuclear reactor), a control responsive to load demand like the turbine input method would be desirable.

As part of the Brayton technology program at Lewis, an alternator load-type speed control was built and tested using solid-state current switching. Figure V-50 shows the experimental transient response of this speed control on a turboalternator. The useful load was switched from full off to full on and then, a few moments later, back to full off. The transient is the most severe that the speed control must accommodate. In the lower trace, it can be seen that, for both load changes, the maximum transient error in frequency was very small, in this case less than 1.5 percent of design frequency of 400 cps and lasting about 0.5 second. The final steady-state error is less than 1 percent. Thus, the alternator load-type speed control is able to maintain speed adequately within close tolerance limits.

The speed control, in effect, matches the alternator power to the turbine power. Matching the system power to the heat source power is now considered.

POWER LEVEL CONTROL

It has been pointed out that control of Brayton system power level is important in order to efficiently convert the power available from the prime heat source to electrical output. The motivation for this control is somewhat different depending on the particular heat source used, that is, isotope, solar, or reactor. The peculiarities of each of these heat sources are shown in figure V-51. For the isotope, the power level decays exponentially with time typical of isotope behavior. For the solar source, the available power oscillates between zero and some maximum as the system orbits the Earth and passes through the Earth's shadow. In the solar system, a heat storage device, the receiver, which is discussed in the Solar Heat Source section, is introduced between the solar source and the conversion system in order to average out the power over the Sun-shade cycles. It is also expected that, over the system lifetime, the net solar input to the system may degrade, because of concentrator surface deterioration, for example.

The reactor is directly controllable in power level; however, it is energy limited and, as figure 51 shows, it may be operated either at a design power level for a fixed period of time or at a reduced power level for a longer period of time.

Before power level matching with these three power sources is discussed, it is necessary first to examine a characteristic that is peculiar to the solar energy source and is due to the requirement for a heat storage device. Figure V-52 illustrates the system behavior for the case where there is a deficit of solar input energy; that is, there is less solar energy per orbit than the system consumes at rated power. Since the receiver (or absorber) concept is to store heat as heat of fusion, the temperature of the storage material will remain constant only as long as the material stays between a fully melted and a fully frozen condition. Where a solar input energy deficit exists, however, the heat storage material will become fully frozen before the end of the shade period and will enter the sensible heat region where the temperature drops rapidly. As a result, the absorber outlet temperature, or turbine inlet temperature, begins to fall and will continue to drop until the sytem reenters the sunlight.

This drop in turbine inlet temperature, with consequent reduction in cycle efficiency, results in a drop in alternator output power, as shown in figure V-52, with a minimum occurring at the end of the shade period. Because of the aforementioned effects, the drop in alternator output with the solar system is more severe than that for the other energy sources, as can be seen in figure V-53.

The solar curve shows that, for a 10 percent decrease in solar input, the alternator output power drops to about 65 percent of rated output at the end of the shade period (fig. V-52). This is obviously an undesirable situation.

For the isotope curve, the alternator power does not drop linearly with source power but has a curvature upward. This trend results from variations in cycle efficiency caused by the combined effects of increasing heat transfer component effectiveness and decreasing turbine inlet temperature as source power decreases, as well as by changes in turbomachinery performance as their operating point changes.

The reactor system does not show any deviation since the power level of the reactor can be independently controlled. However, as mentioned in the alternator speed control section, it would be desirable to be able to efficiently throttle back on reactor power when it is not needed in order to extend the lifetime of the system. These three curves (fig. V-53) indicate that some means of controlling system power level would be highly desirable.

Analog computer system studies were undertaken to determine the most effective control for this purpose. The dashed curve in figure V-53 shows the benefits resulting from the use of a system pressure level control to match the system power demand to the available heat source power. Relative system pressure level is shown as a parameter along the curve. Through the use of such a pressure control, a 20 percent decrease in heat source power can be accommodated with a decrease in alternator power of less than 10 percent. For the solar source, the use of a system pressure level control results in maintaining the receiver in the heat of fusion region at all times. For the isotope source, it is a means of maintaining turbine inlet temperature as power degrades, thus maintaining high cycle efficiency. For the reactor, it is a means of efficiently reducing power demand in order to extend operating time.

While figure V-53 shows data for a two-shaft Brayton system, preliminary investigations of a one-shaft configuration have shown a similar benefit from pressure control. Thus, Lewis computer studies have shown that system pressure control is an effective means of matching the Brayton conversion system to the power source.

On the basis of the results of analog studies, it has been concluded that there is no fundamental reason that will prevent adequate control of the Brayton power system. However, work on system hardware is just getting underway, and problems may still arise.

SYSTEM START

The final item of system technology to be discussed is system start. The method of start is, of course, dependent on the particular system configuration. For a two-shaft Brayton system, various start procedures have been studied using an analog computer dynamic system simulation. The start method finally chosen utilized an injection of the cycle gas through the turbine into the evacuated system to bring the turbocompressor up to speed. This method requires some peripheral equipment shown in figure V-54. In this figure, the solar Brayton configuration is illustrated as an example, and the peripheral components are indicated by the numbers: (1) A primary heat source control, to start the system, is given the command to bring the source to working temperature. (2) The alternator field must be externally powered during start to ensure that electrical power will immediately be available to control speed. (3) The application of jacking gas to lift off the gas bearing occurs next for the turboalternator and turbocompressor. The bearings are operated hydrostatically until the rotating units are up to speed; (4) The gas bottle and injection valve, the isolation valve to prevent back flow during gas injection, and the exhaust valve used to evacuate the system are shown.

Various start procedures have been studied, including various injection flow rates and with and without the system exhaust valve open. These studies show that, because of the volume of the heat exchanger components, the system can be started successfully at 20 percent of rated flow with the exhaust to space valve closed. This particular start procedure is shown in figure V-55. Note the expanded insert on the time axis for a 1 minute period during the start. Time zero is taken, using the solar Brayton system as an example, as the moment the system enters the sunlight.

The step by step sequence is as follows: once in orbit, the system is given the command to bring the primary heat source up to temperature, in this case, to bring the absorber melt quality to 1.0 as shown by the top trace. After an appropriate period of time, injection of gas inventory into the system is begun, as shown by the second trace. The isolation valve is closed at this time to prevent backflow of the injected gas. The gas exits from the absorber and enters the turbine at rated temperature, bringing the turbocompressor up to speed in about 15 seconds. At some point in the turbocompressor speedup, the compressor discharge pressure exceeds the injection pressure downstream of the isolation valve, and the valve is driven full open. The compressor flow then adds to the injection flow, and the system bootstraps itself up to rated conditions. The turboalternator speedup follows the turbocompressor speedup with the speed control taking over when the alternator reaches rated frequency. The turboalternator power overshoots, however, for about the first 30 minutes of operation because of initially cold radiator and, therefore, higher cycle efficiency.

The single-shaft Brayton system may be also started in the manner just described. In addition, however, it may be possible to start the single-shaft system by running the alternator as a motor on an inverter from battery power. This start scheme has not been fully studied as yet.

As part of the Lewis in-house study of Brayton systems, a breadboard loop has been built into which the turbocompressor discussed herein has been placed. Progress in this program has been made to a point where the system has been started through closed-loop injection several times. One such time history of a start sequence is presented in figure V-56. At the 2-second point, the injection valve was opened, forcing the gas through the heater and turbine and spinning it up rapidly to over 17 000 rpm. At the 4-second point, the isolation valve was opened, permitting the gas to circulate through the loop. The temperature level into the turbine had risen to 1100° R in the meantime. This temperature is insufficient for self-sustained operation so the speed is noted to drift off. However, the inlet temperature continued to rise as rig parts approached equilibrium temperatures and, at the 50-second point, it had risen to 1250° R where it was sufficient for development of net work from the system. From this point on, the turbocompressor proceeded to accelerate in a self-sustained manner up to equilibrium speed. The equilibrium speed ultimately reached was approximately 25 000 rpm. These results are very encouraging, and it appears that the start of a Brayton system should be a rather straightforward process with the prospect of closed-loop starting being reasonably good.

CONCLUDING REMARKS

From the Brayton technology discussion it is evident that this type power system embodies a wide variety of technology areas. Although all cannot be summarized, some of the major points brought out can be reviewed.

1. From the cycle discussion, it was indicated that relatively large radiator areas are required. This factor, together with the high potential cycle efficiency, results in the principal emphasis being placed on low and intermediate power level applications where cycle performance dominates. Also it was indicated that working fluid pressure levels and the use of inert gas of varying molecular weights are extremely valuable tools in the selection of optimum component geometry for a given application.

2. From the component investigations to date, it can be concluded that acceptable performance can be obtained, particularly with respect to the most critical turbomachinery involved. The gas bearing program has indicated that they work stably and with acceptable loss. From the packaging program, control of the internal thermal conditions appears to be of major concern.

3. The system studies have indicated that control of pressure level through inventory modulations is an extremely valuable tool in the control of power output. Starting studies have also

indicated that this aspect of operation should be relatively straightforward.

It should be emphasized that there is still much ground to cover before the assessment of the Brayton system is complete. The package program, for example, has not progressed to a point where major conclusions regarding mechanical integrity and life can be drawn. The study of magnetic unbalance in the alternator component and its effect on gas bearing design and operation has only begun. It was also indicated herein that much progress must still be made in the area of the heat sources. Thus, it is evident that, although substantial advances have been made and results obtained to date are encouraging, considerable effort is still required before ultimate conclusions can be recorded regarding the Brayton cycle for space power.

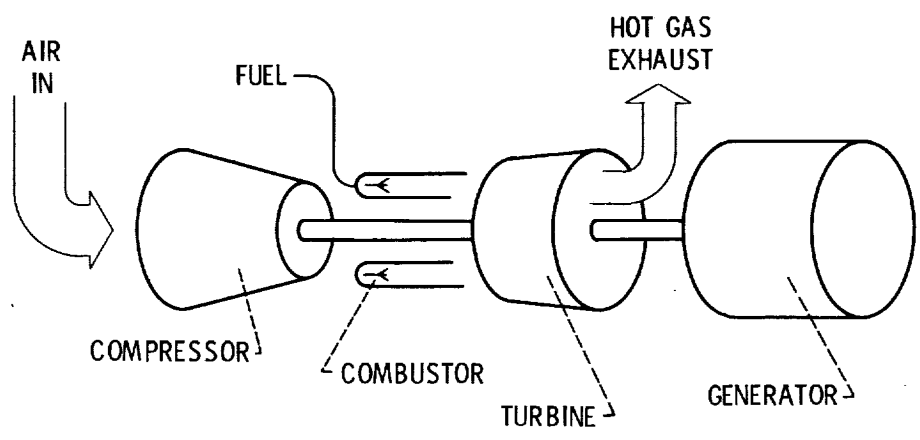

Figure V-1. - Gas turbine Brayton power system.

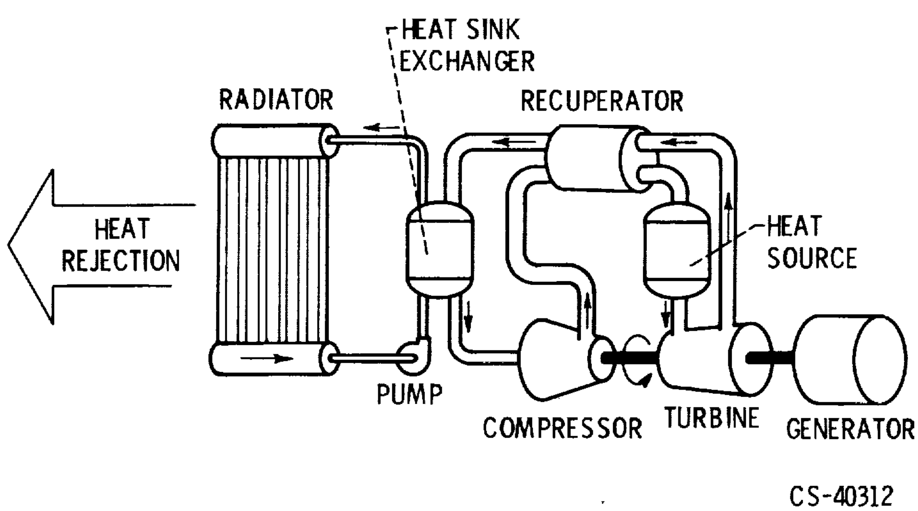

Figure V-2. - Brayton cycle space power system.

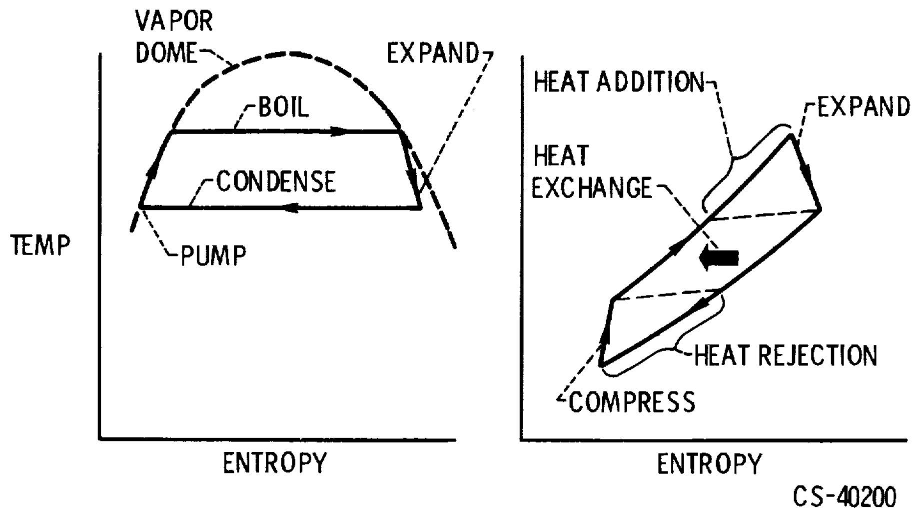

(a) Rankine system. (b) Brayton system.

Figure V-3. - Cycle thermodynamic comparison.

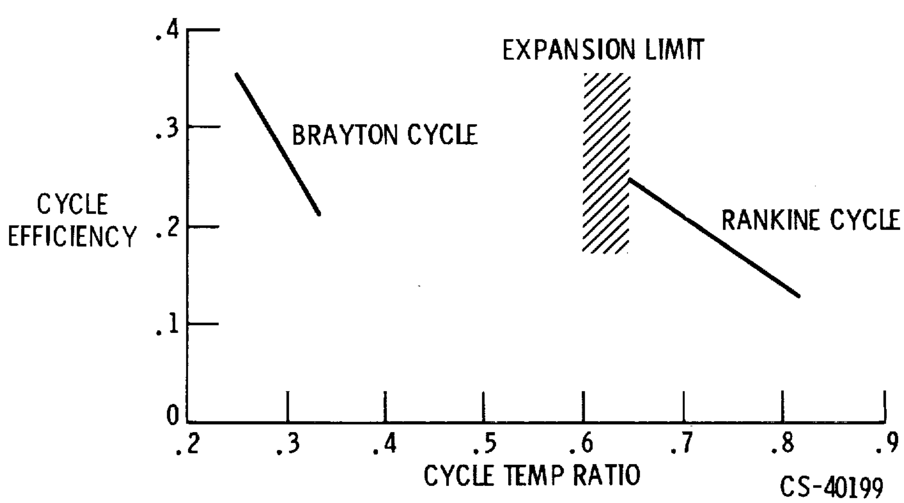

Figure V-4. - Cycle efficiency comparison.

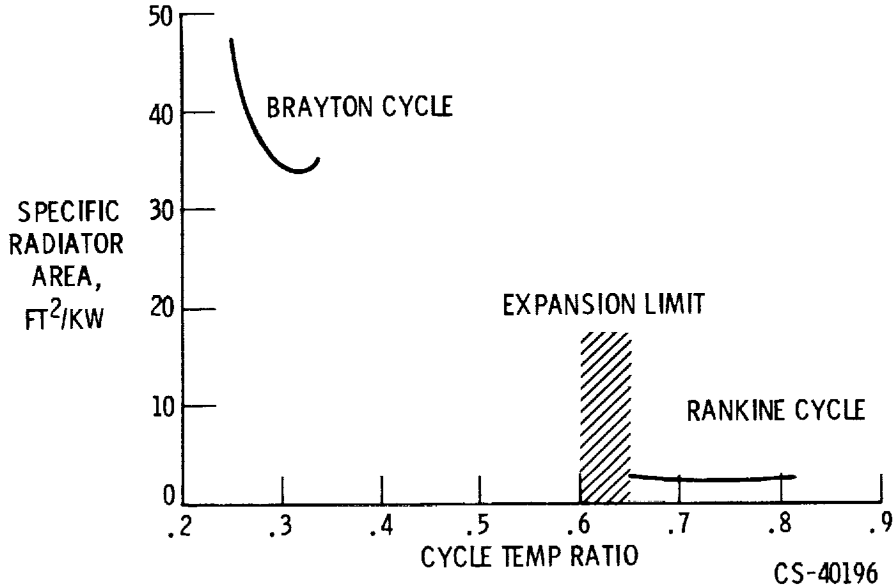

Figure V-5. - Radiator area comparison. Turbine inlet temperature, 1950^{0} R; sink temperature, 400^{0} R.

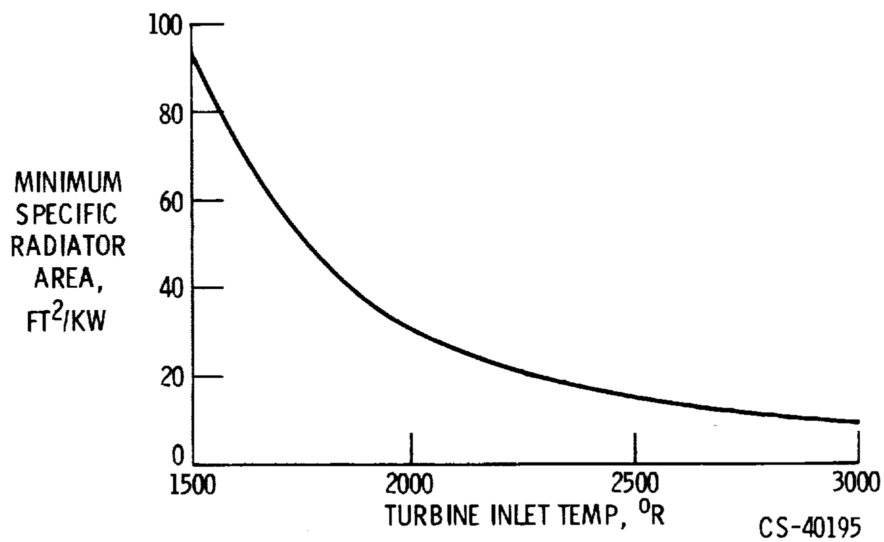

Figure V-6. - Effect of turbine-inlet temperature on radiator area. Sink temperature, 400^{0} R.

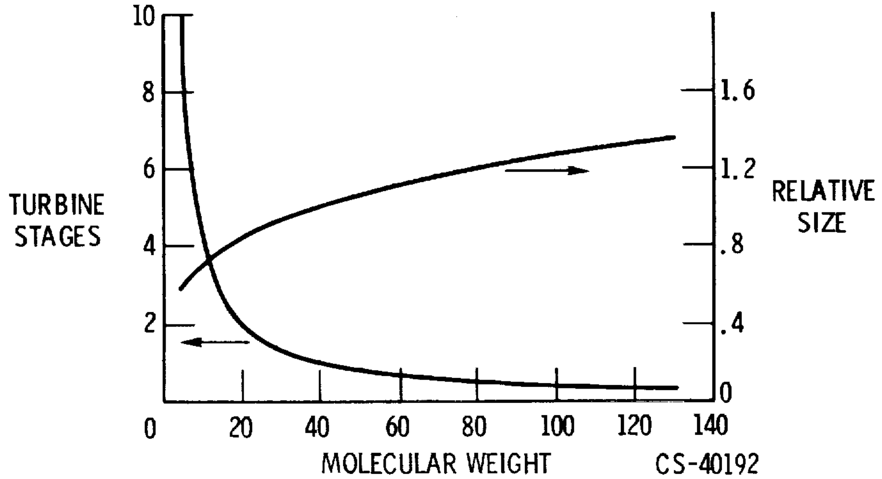

Figure V-7. - Effect of molecular weight on turbomachinery.

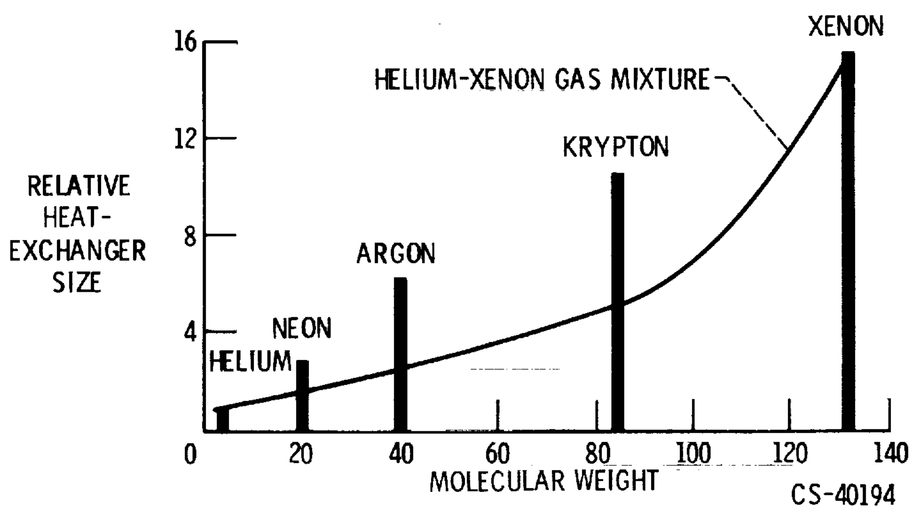

Figure V-8. - Effect of molecular weight on heat-exchanger size.

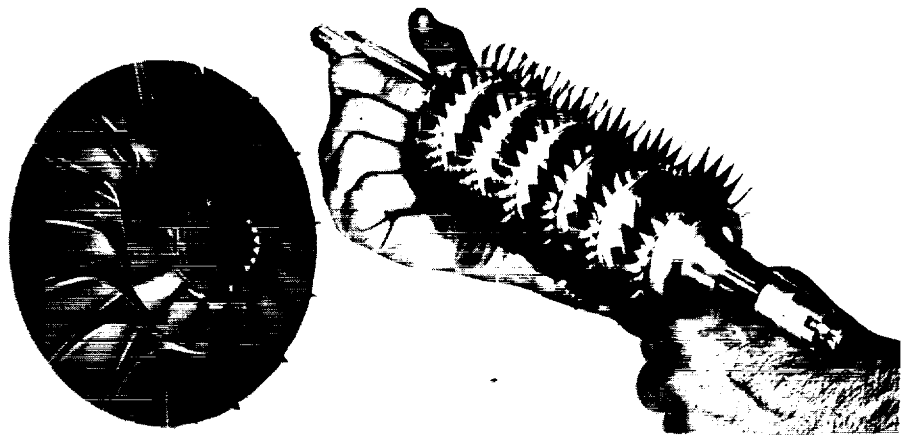

CS-40274

(a) Centrifugal. (b) Axial.

Figure V-9. - Brayton-cycle compressors.

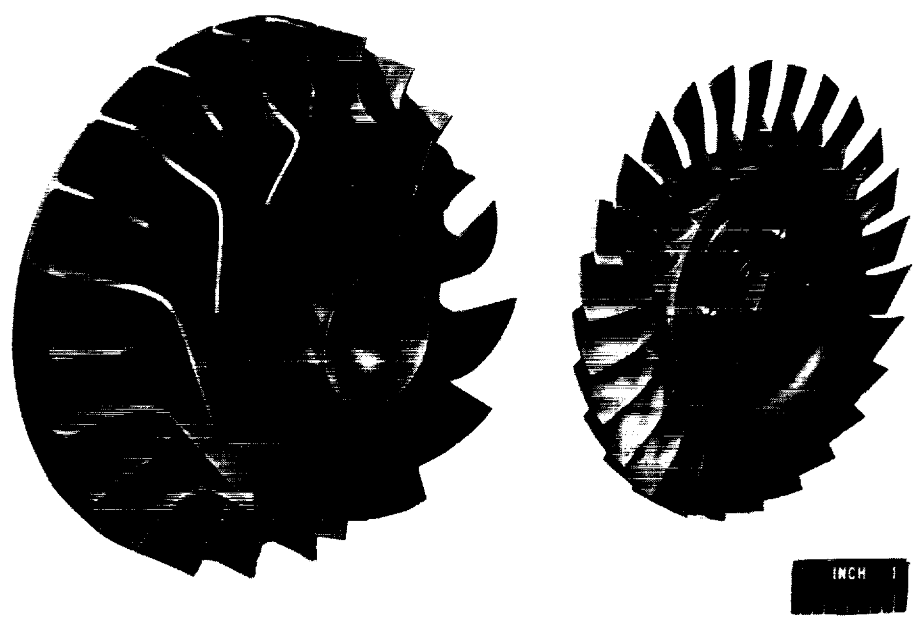

CS-40265

(a) Radial. (b) Axial.

Figure V-10. - Brayton-cycle turbines.

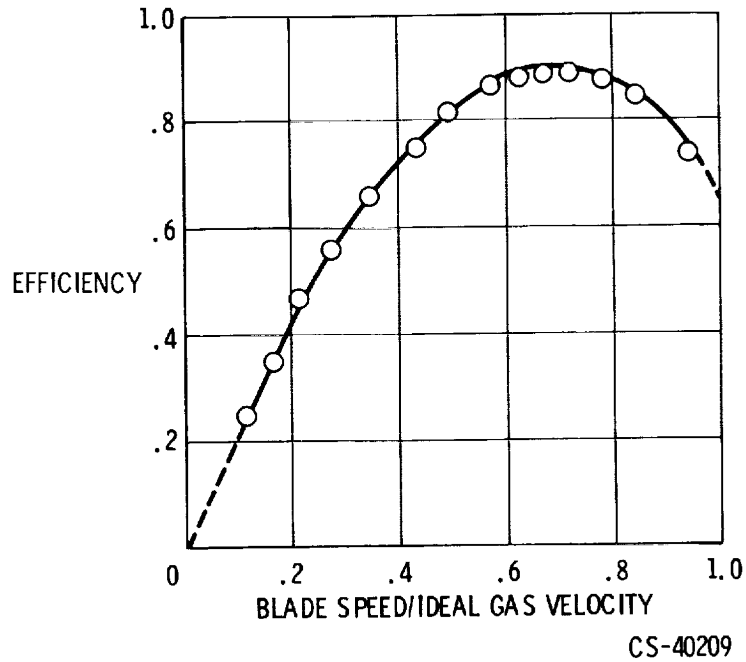

Figure V-11. - Radial turbine performance. Diameter, 6 inches; fluid, argon.

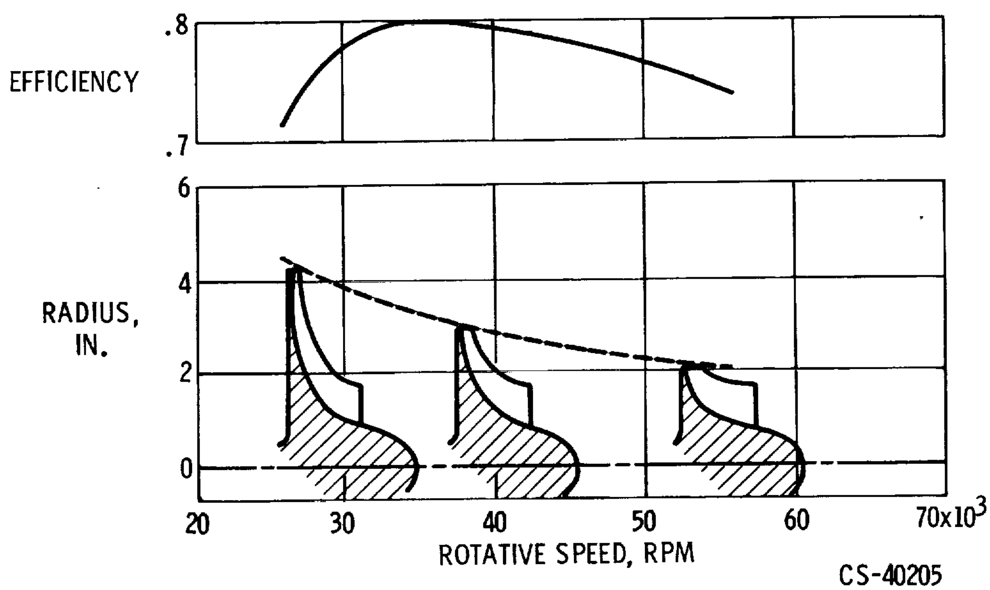

Figure V-12. - Centrifugal compressor efficiency - geometry relation.

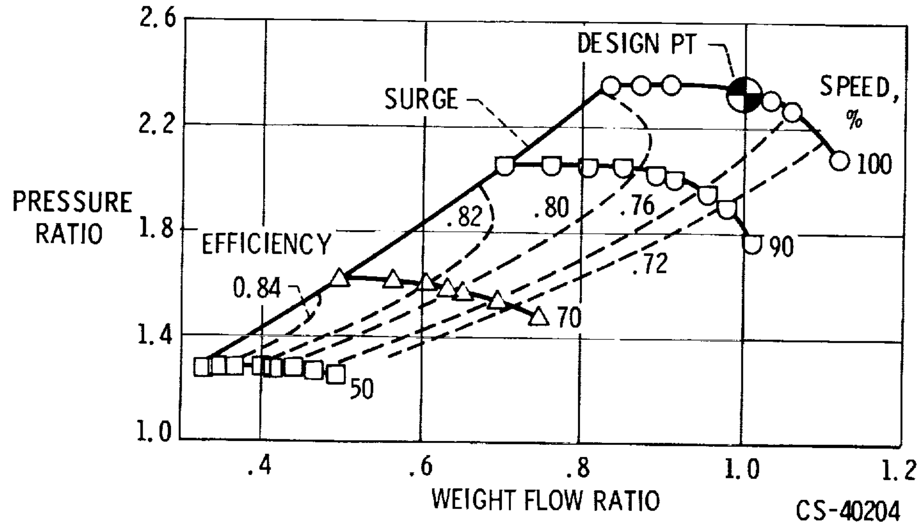

Figure V-13. - Centrifugal compressor performance. Diameter, 6 inches; fluid, argon.

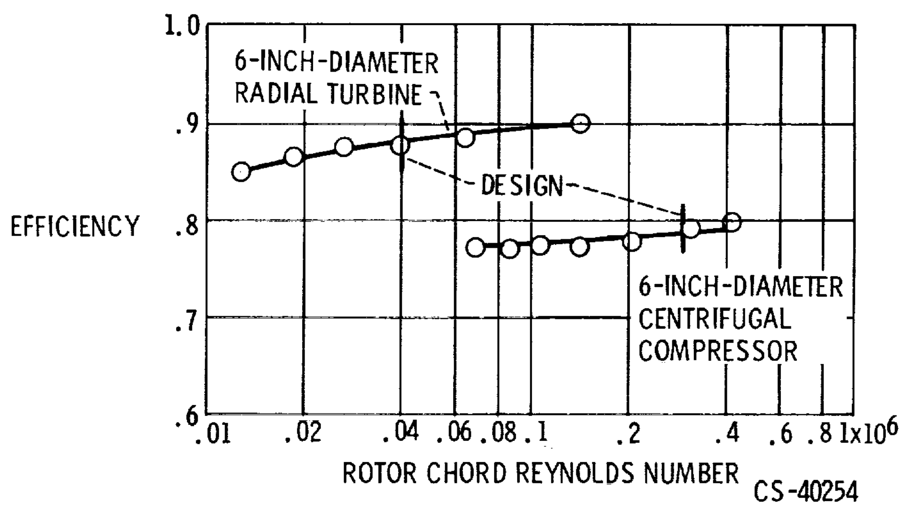

Figure V-14. - Effect of Reynolds number on efficiency. Turbine fluid, argon; compressor fluid, air.

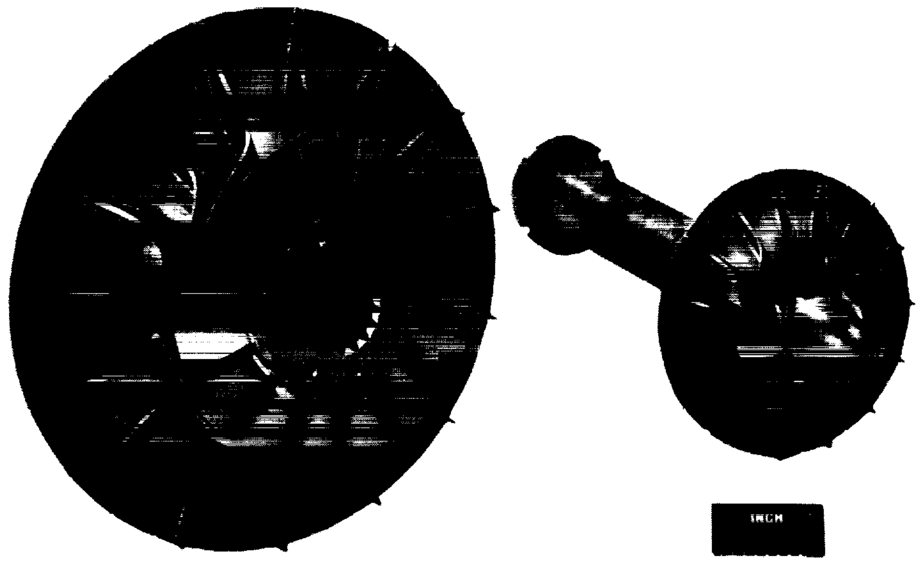

CS-40268

(a) 6.0-Inch diameter. (b) 3.2-Inch diameter.

Figure V-15. - Compressors for size effect study.

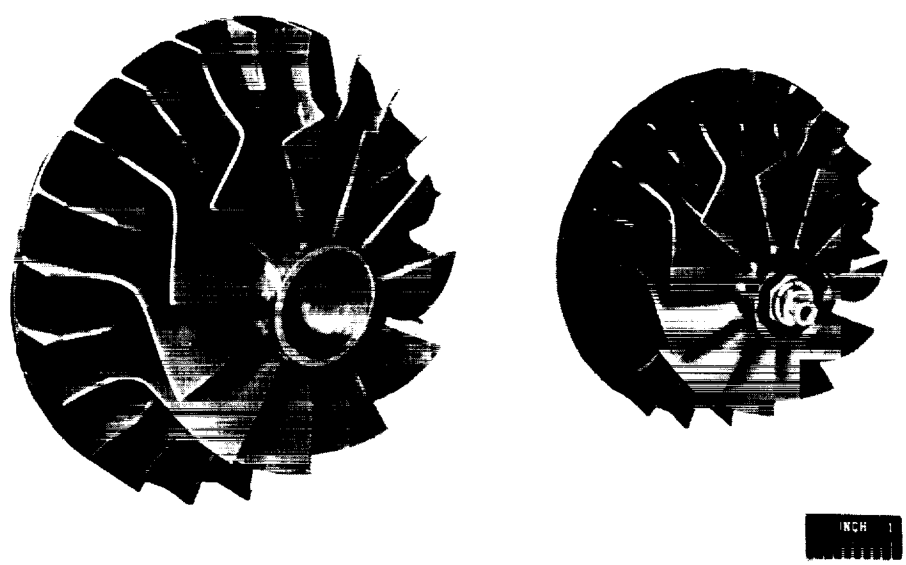

CS-40267

(a) 6.0-Inch diameter. (b) 4.6-Inch diameter.

Figure V-16. - Turbines for size effect study.

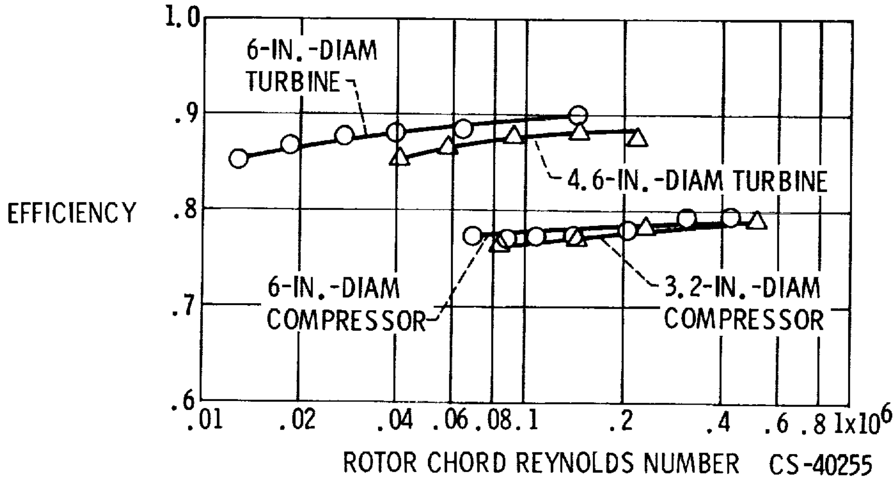

Figure V-17. - Effects of Reynolds number and size on efficiency. Turbine fluid, argon; compressor fluid, air.

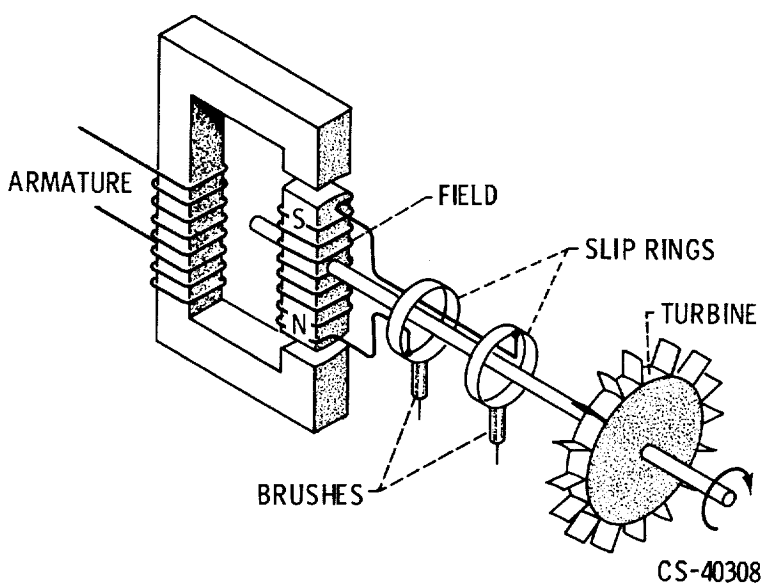

Figure V-18. - Conventional wound rotor alternator.

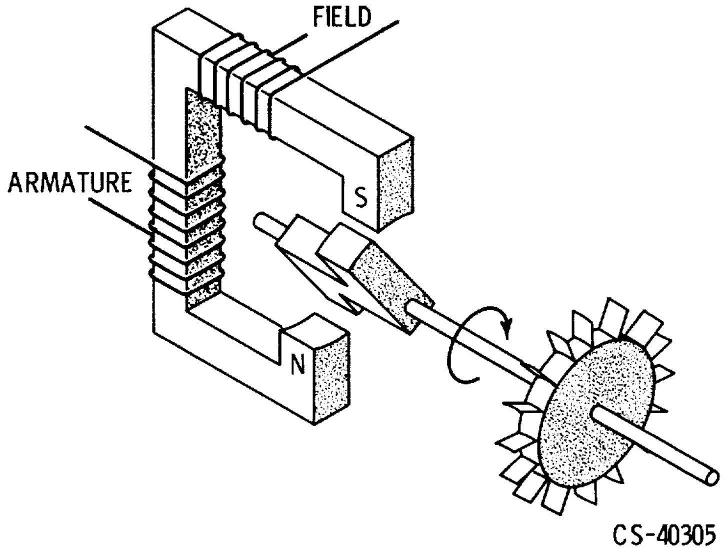

Figure V-19. - Brushless solid rotor alternator.

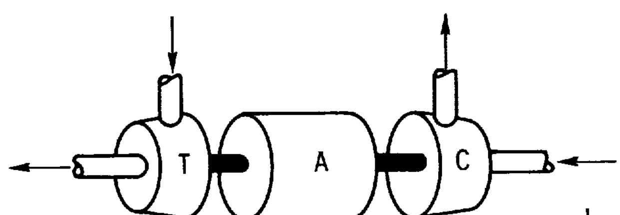

(a) Single-shaft system; high-speed alternator.

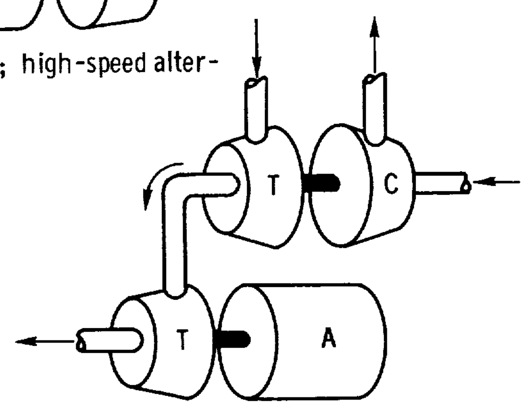

(b) Two-shaft system; low-speed alternator.

Figure V-20. - Shaft arrangements.

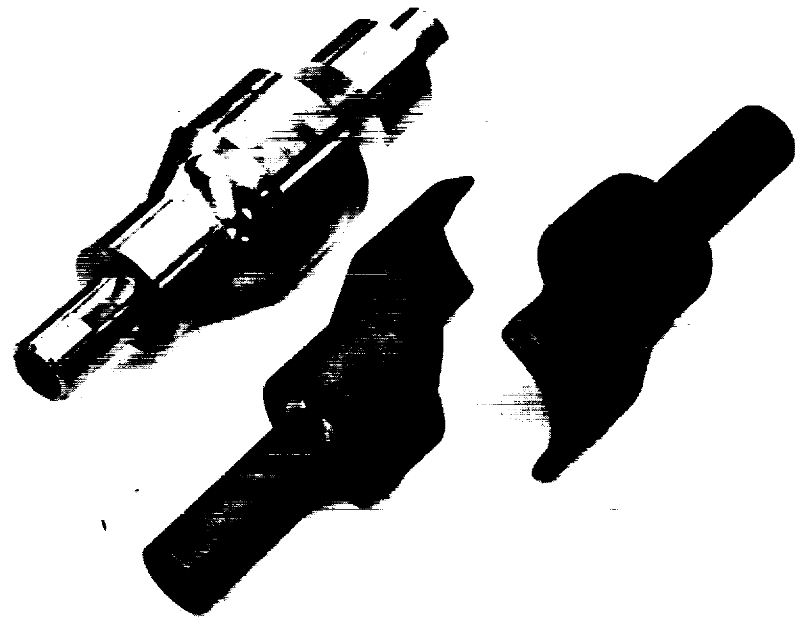

Figure V-21. - High-speed solid rotor.

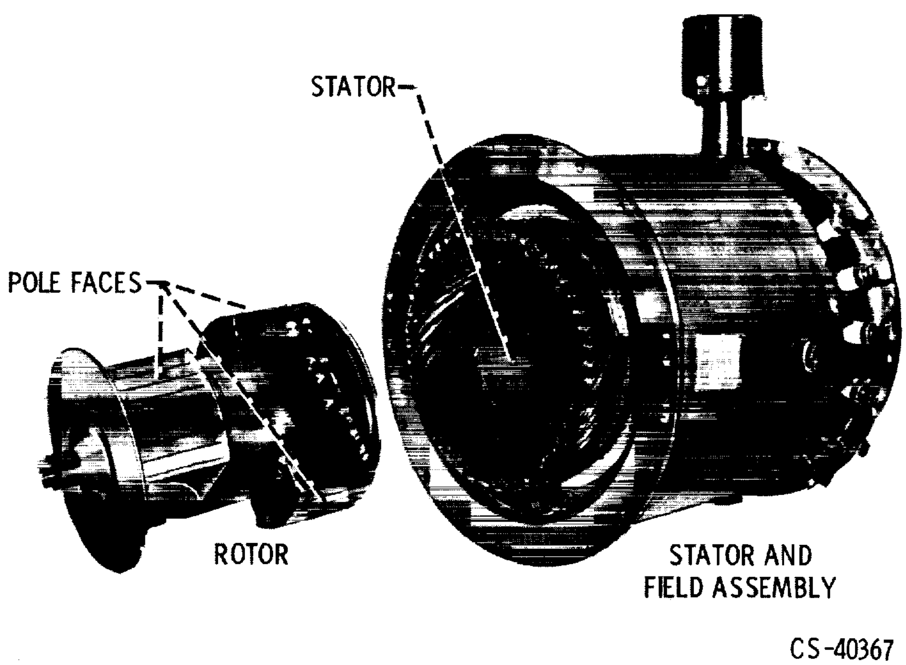

Figure V-22. - Brayton solid rotor alternator.

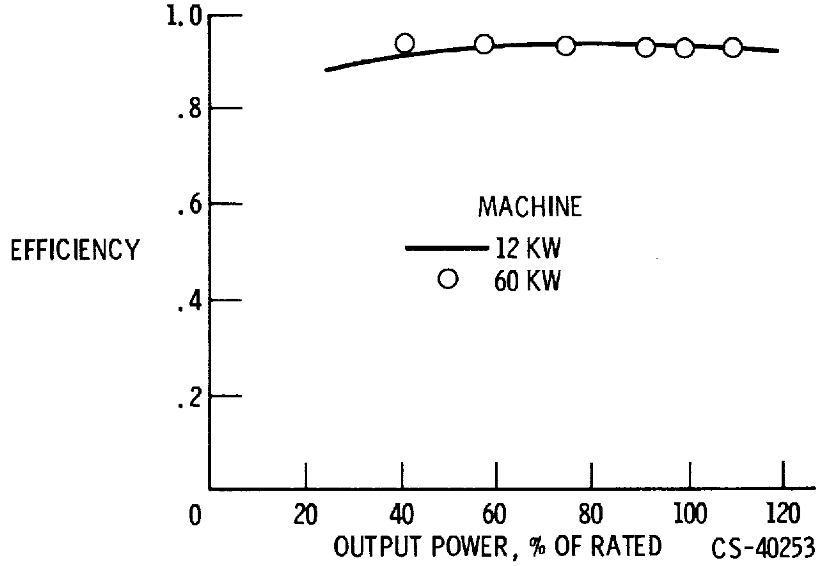

Figure V-23. - Solid rotor alternator performance. Power factor, 0.8.

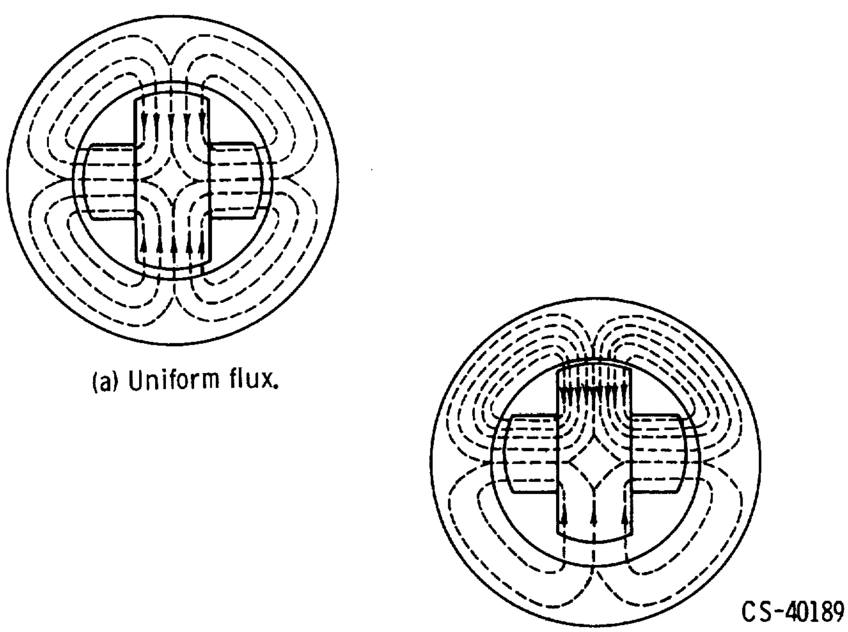

(a) Uniform flux.

(b) Distorted flux.

Figure V-24. - Magnetic unbalance.

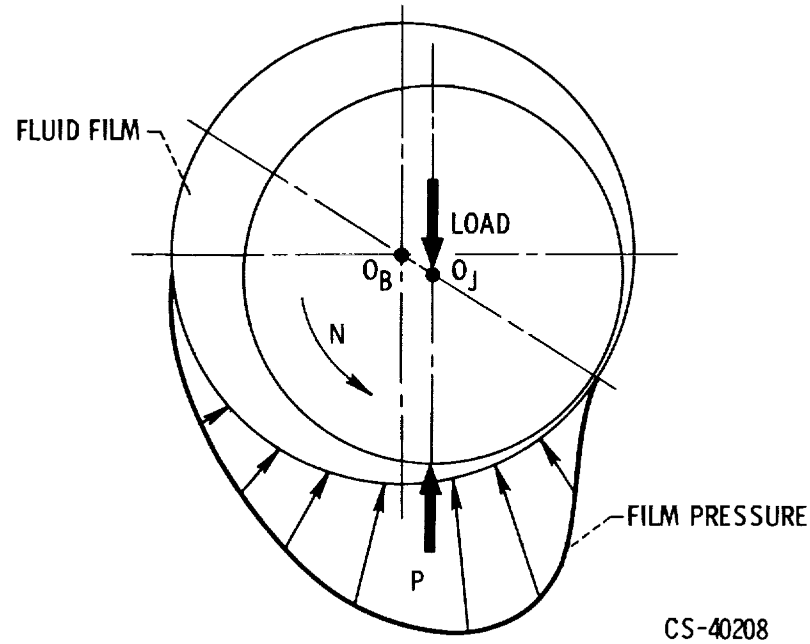

Figure V-25. - Journal bearing.

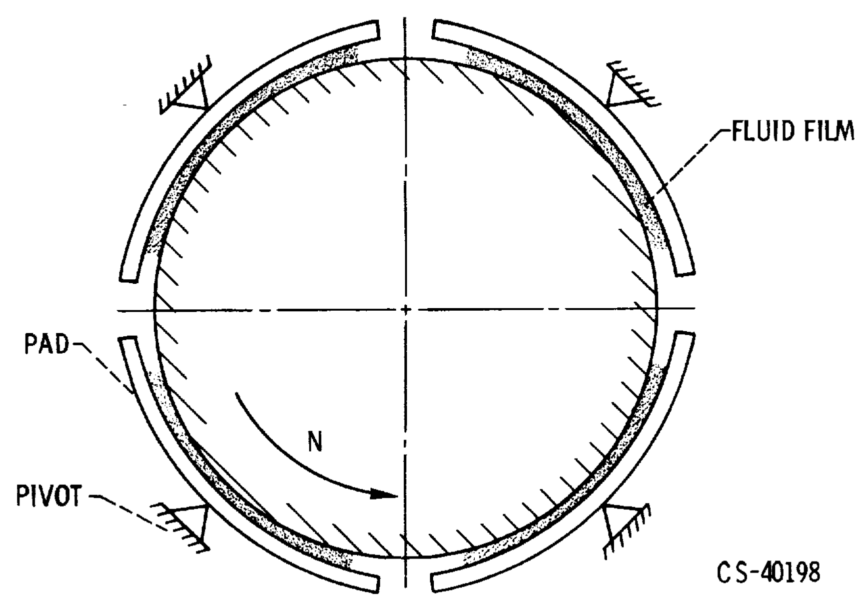

Figure V-26. - Pivoted pad journal bearing.

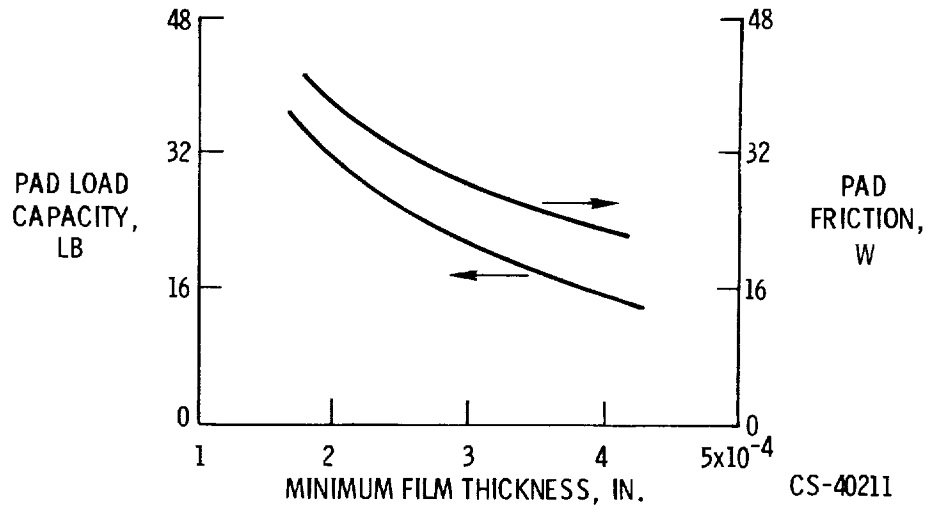

Figure V-27. - Typical journal bearing pad performance.

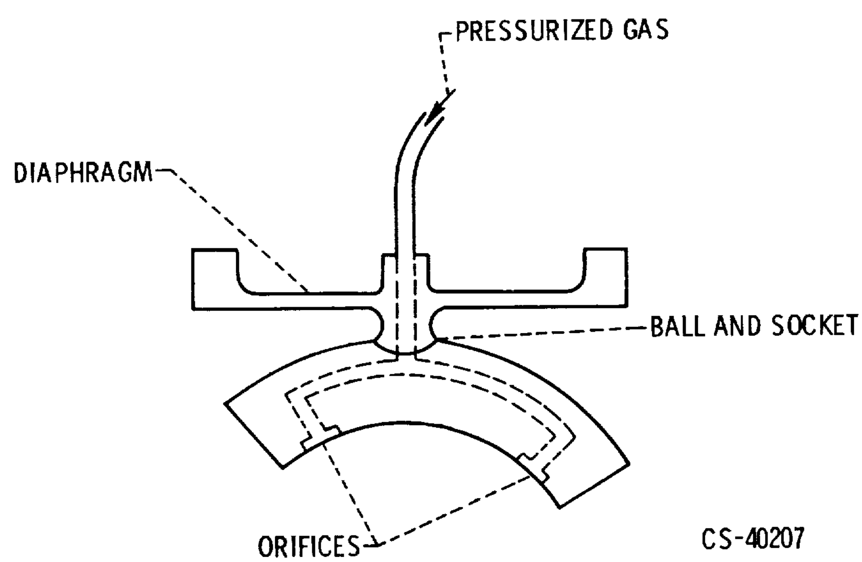

Figure V-28. - Pivot and external pressurization arrangement.

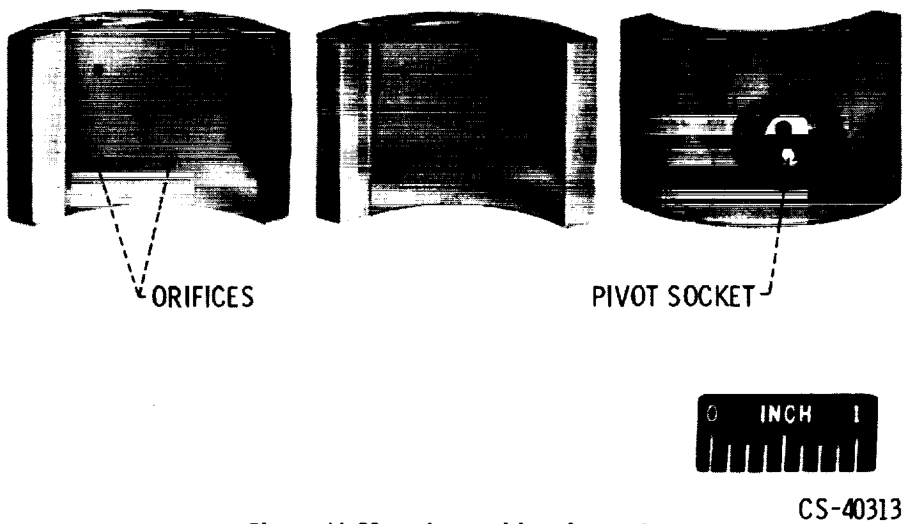

Figure V-29. - Journal bearing pads.

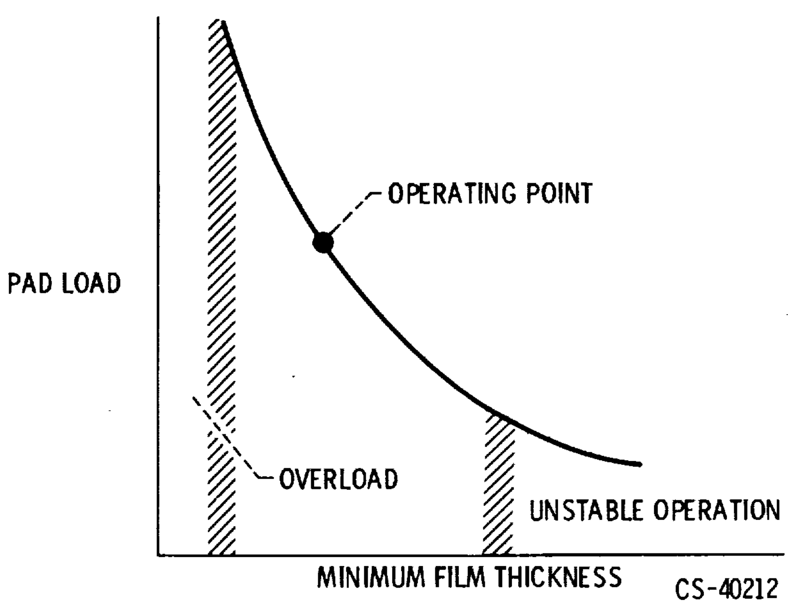

Figure V-30. - Pad loading at various film thicknesses.

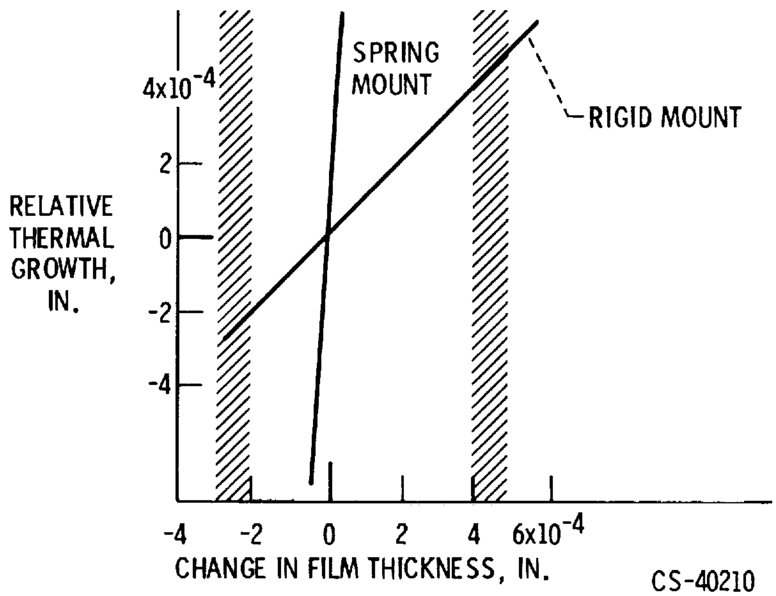

Figure V-31. - Effect of pad mount stiffness on thermal tolerance.

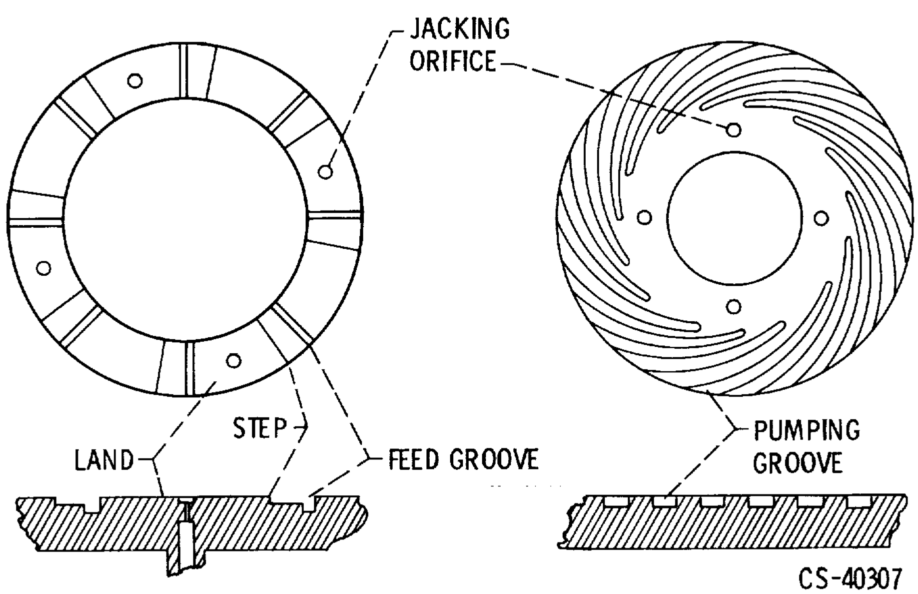

(a) Rayleigh step.

(b) Spiral groove.

Figure V-32. - Thrust bearing types.

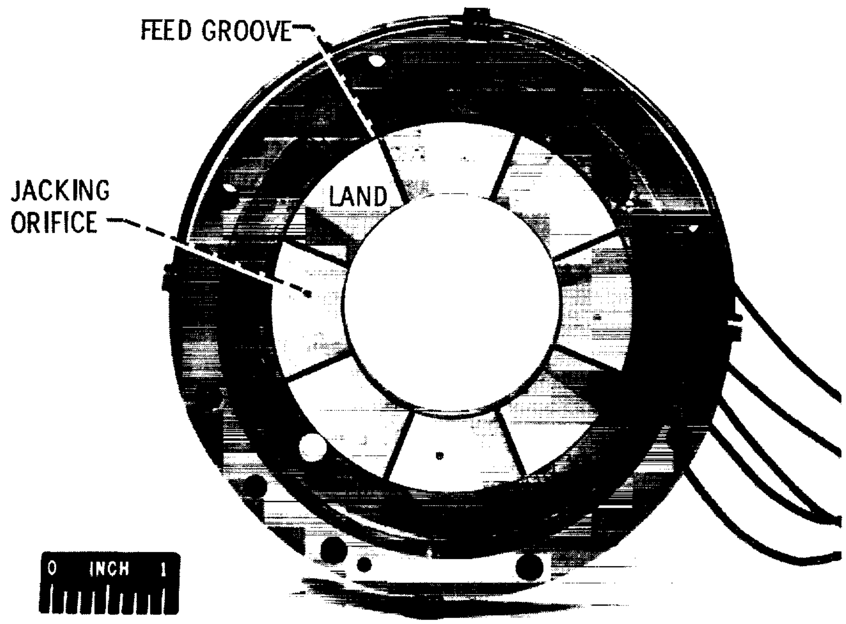

CS-40272

Figure V-33. - Rayleigh step thrust bearing.

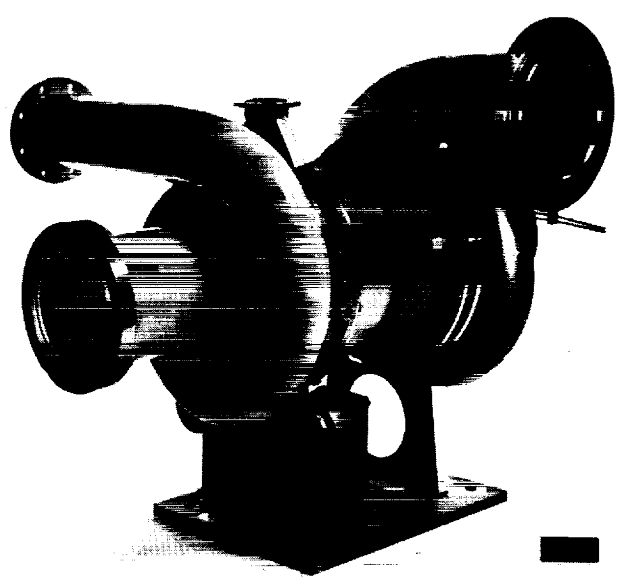

CS-40271

Figure V-34. - Research turbocompressor.

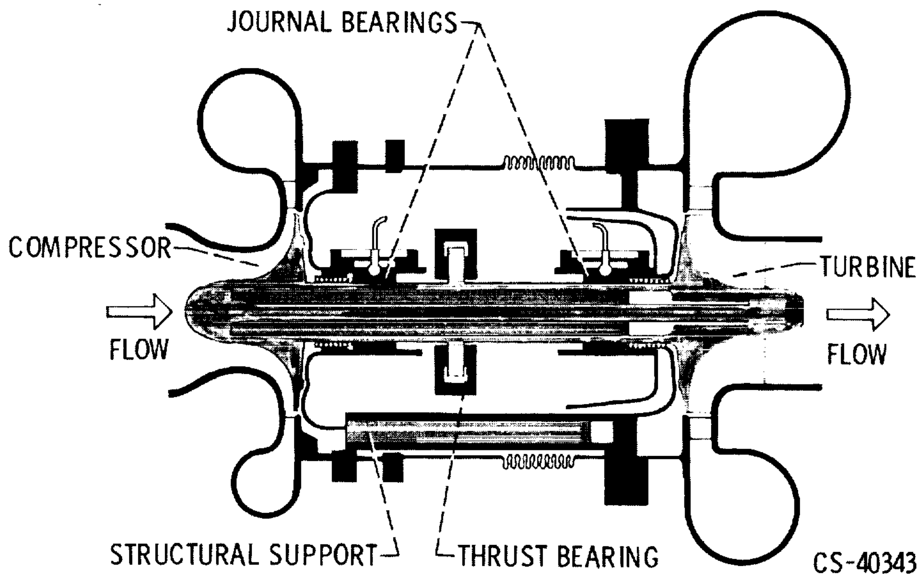

Figure V-35. - Schematic of turbocompressor.

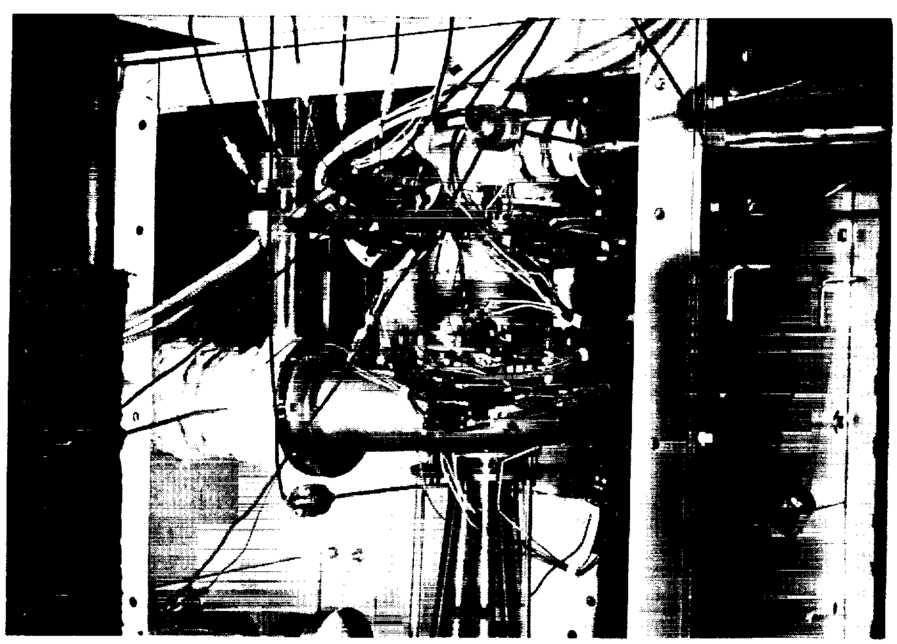

CS-40202

Figure V-36. - Turbocompressor installation.

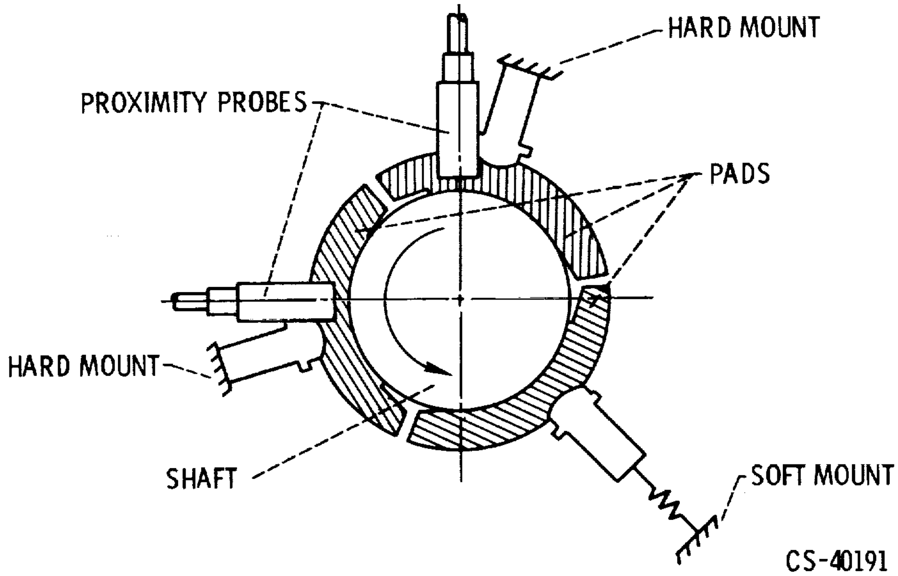

Figure V-37. - Journal bearing arrangement.

Shaft speed, rpm x 10^2

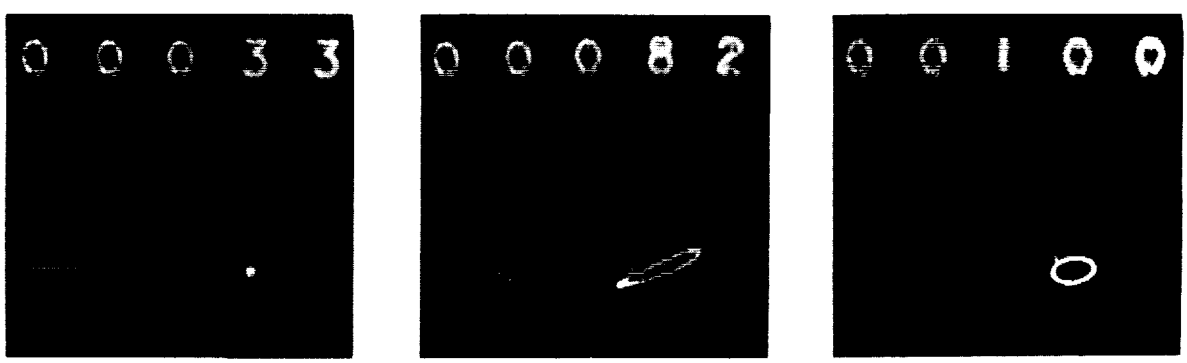

(a) No eccentricity. (b) 0.001-Inch ellipse. (c) 0.0005-Inch circle.

Figure V-38. - Shaft orbit patterns. CS-40171

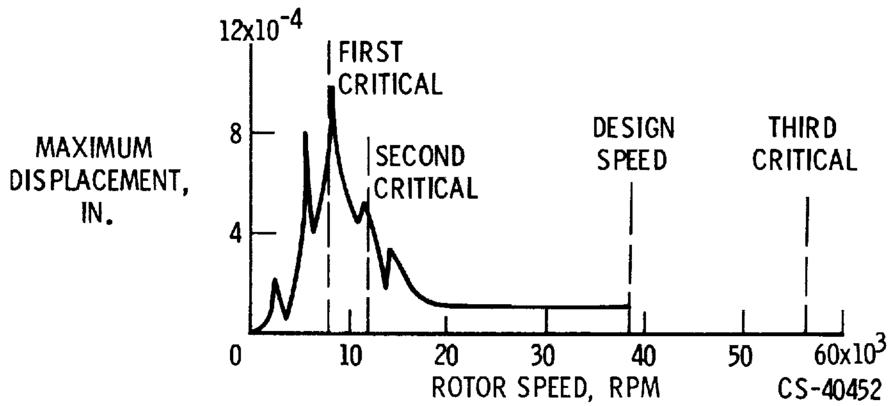

Figure V-39. - Turbocompressor shaft displacement.

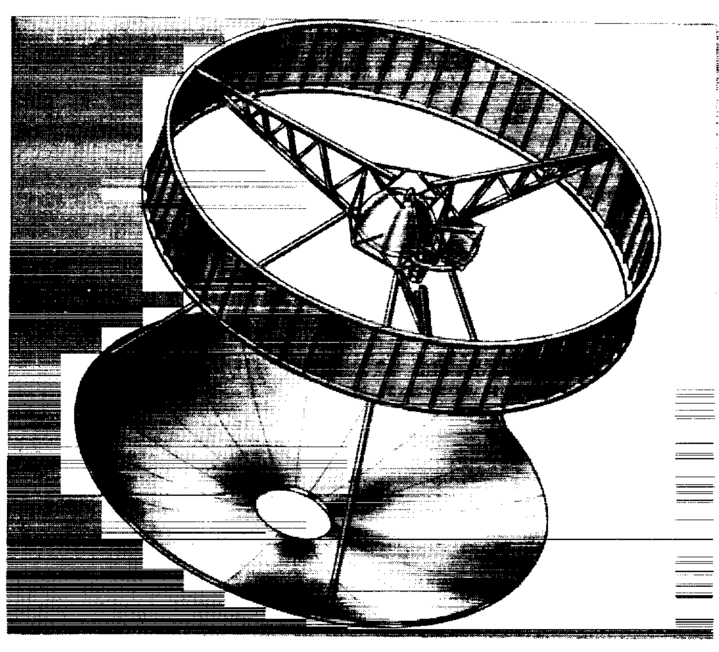

CS-40201

Figure V-40. - Solar Brayton cycle space power system.

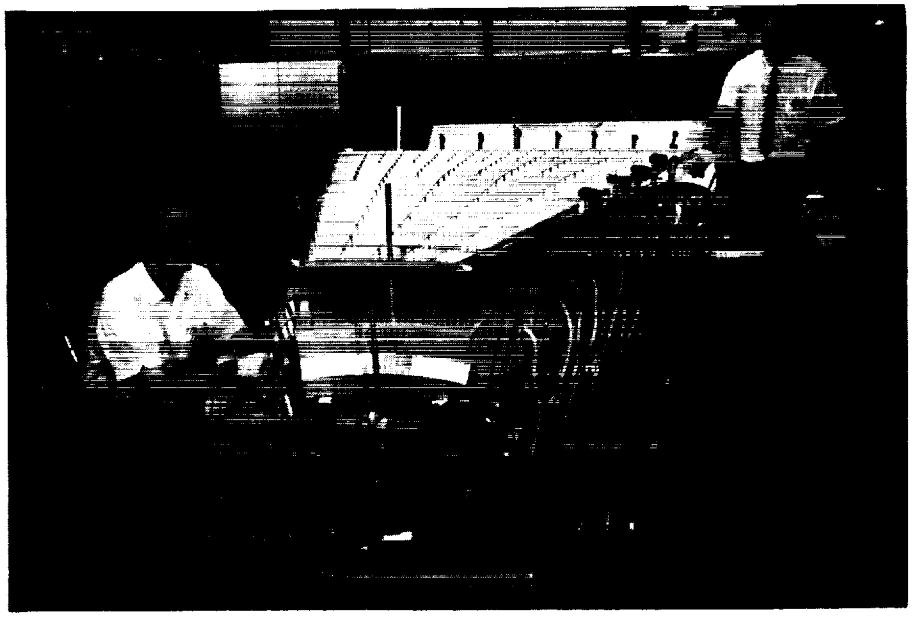

CS-40263

Figure V-41. - Formation of concentrator sector.

CS-40264

Figure V-42. - Ribbed back of 20-foot concentrator.

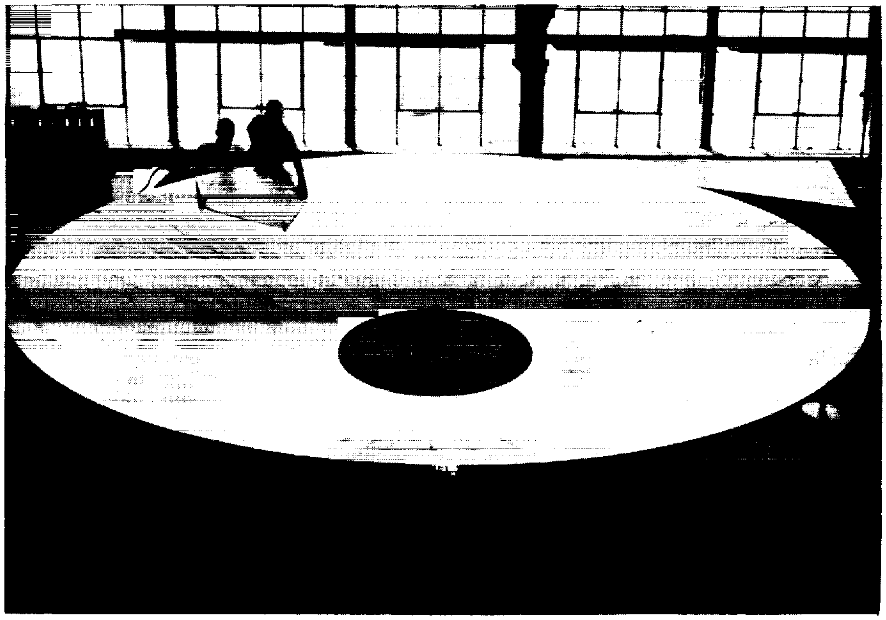

CS-40270

Figure V-43. - Polished front of 20-foot concentrator.

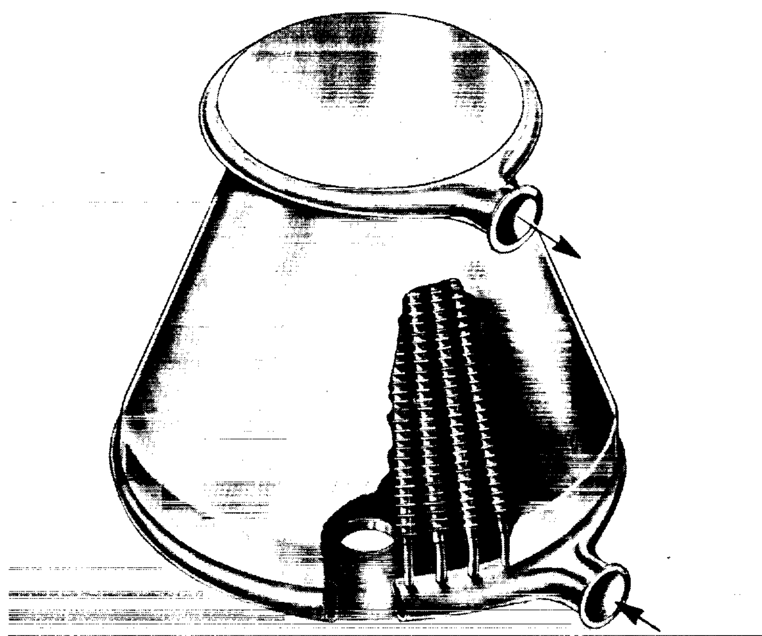

CS-40368

Figure V-44. - Heat receiver.

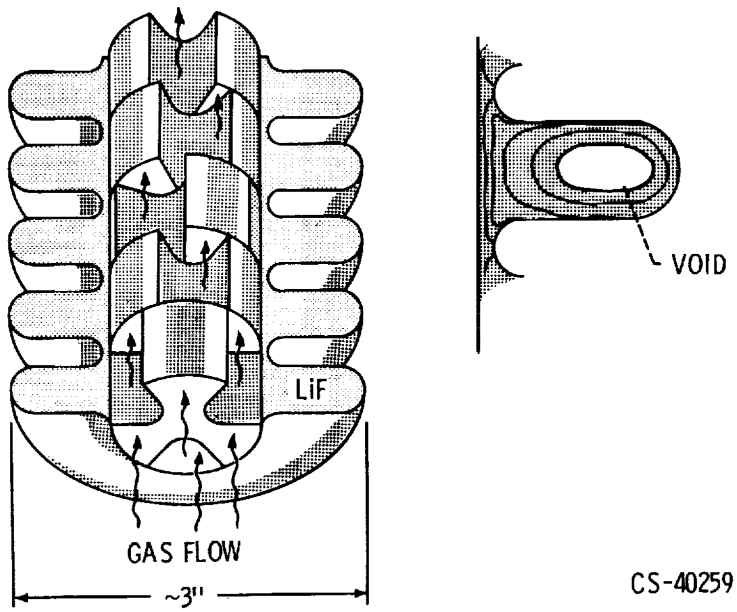

(a) Cutaway of tube.

(b) Expected freeze pattern.

Figure V-45. - Receiver tube concept.

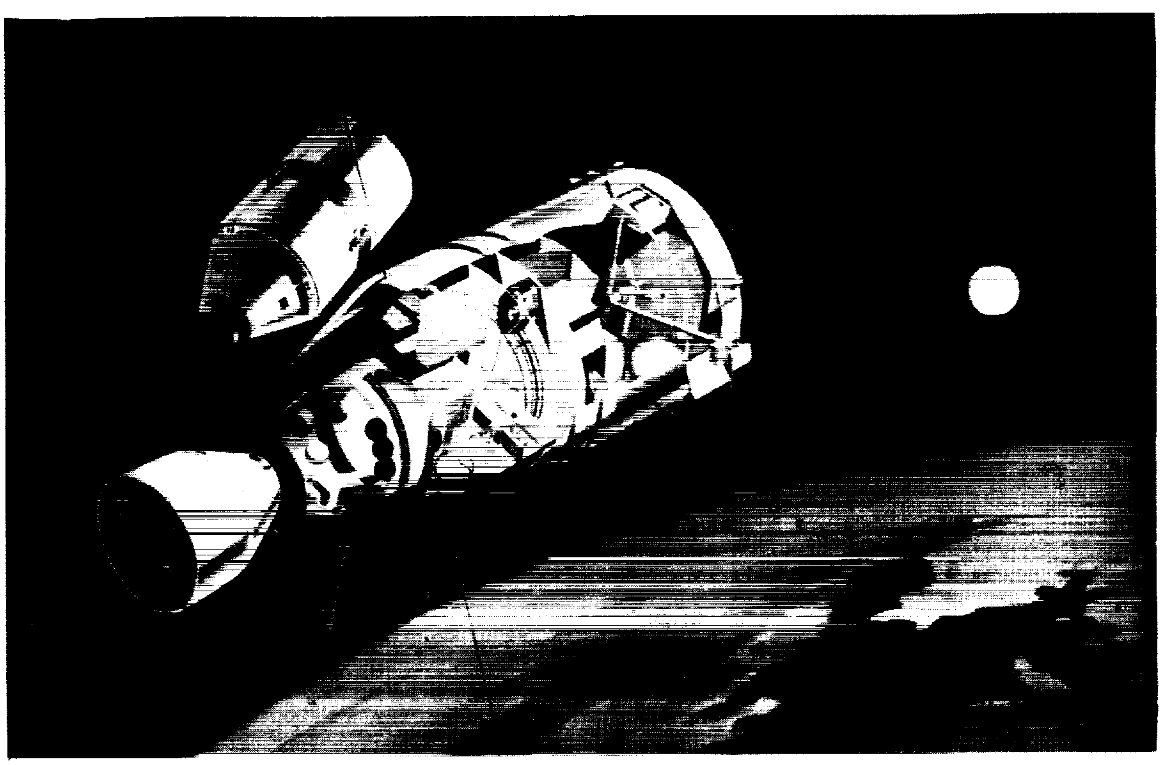

CS-39850

Figure V-46. - Isotope Brayton space station concept.

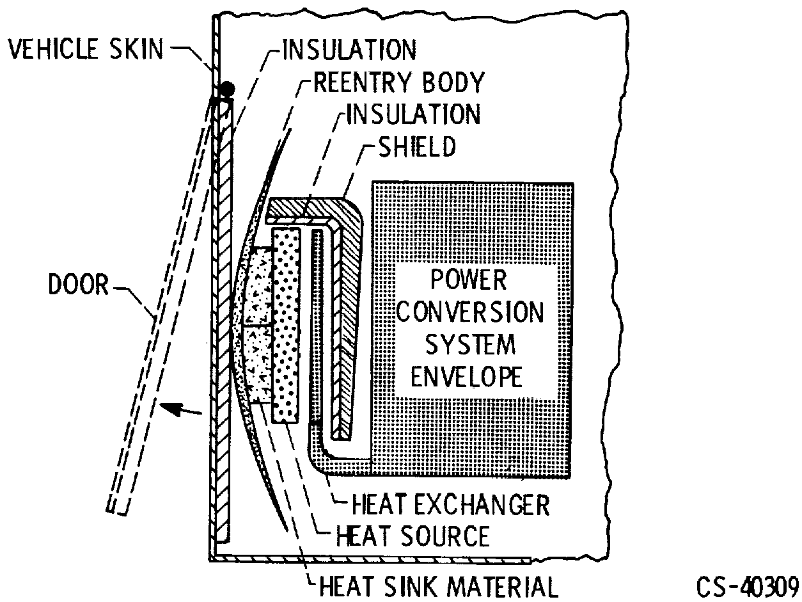

Figure V-47. - Radioisotope Brayton cycle concept.

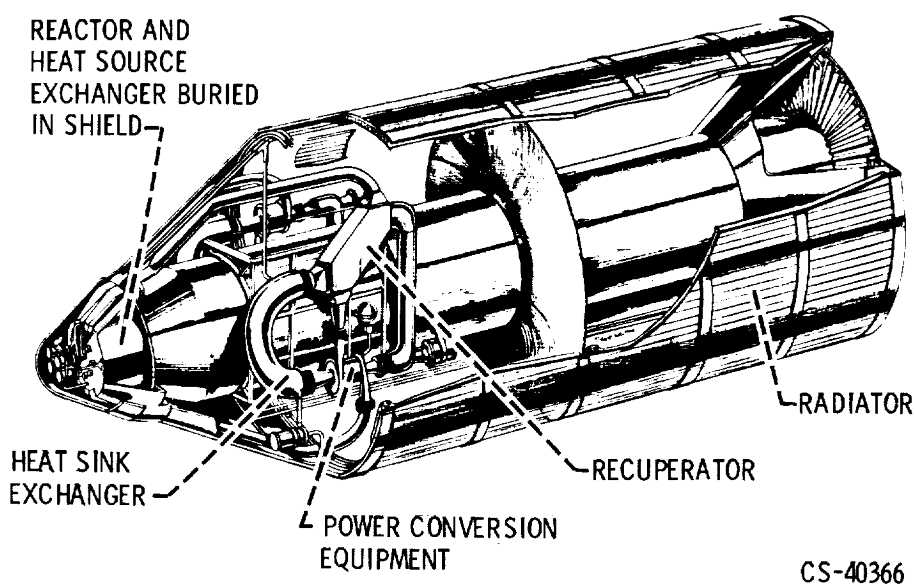

Figure V-48. - 150-Kilowatt-electric nuclear Brayton system.

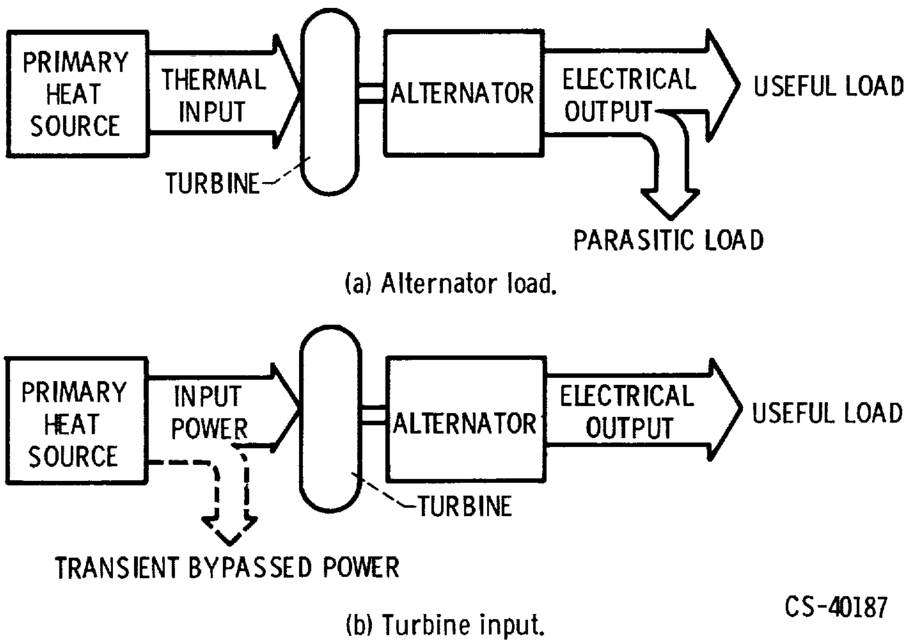

Figure V-49. - Speed control techniques.

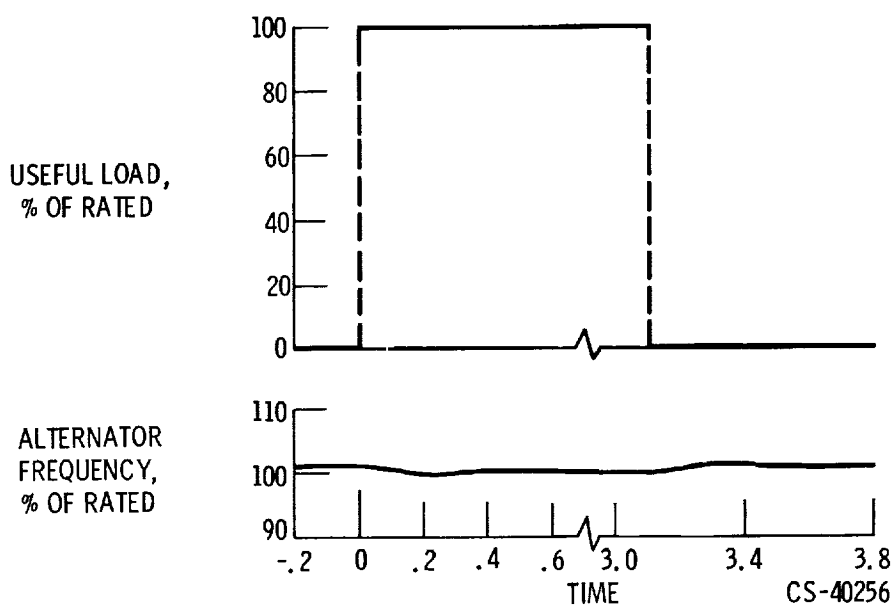

Figure V-50. - Experimental performance of speed control.

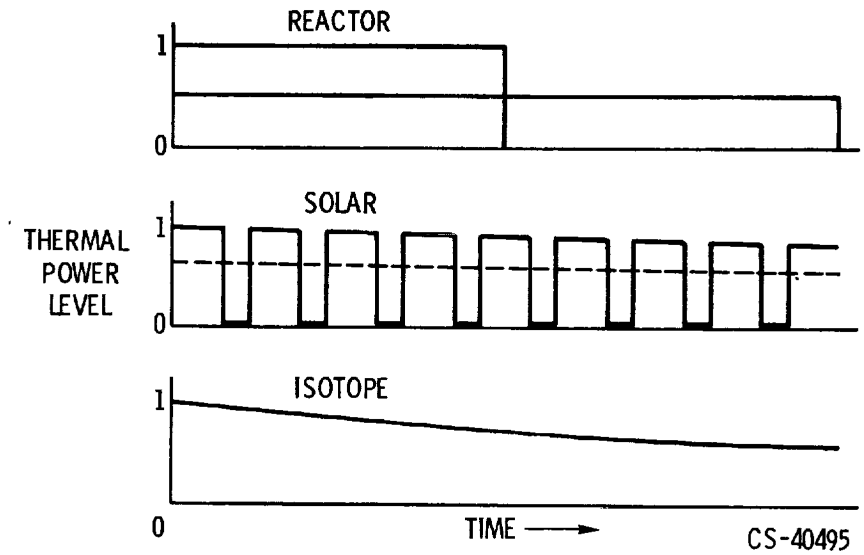

Figure V-51. - Heat-source characteristics.

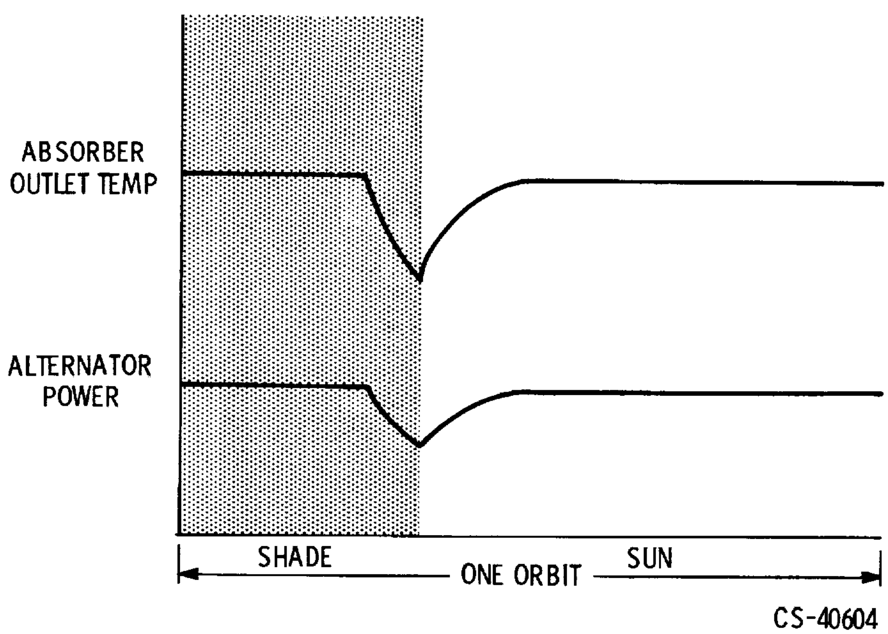

Figure V-52. - Energy imbalance effects.

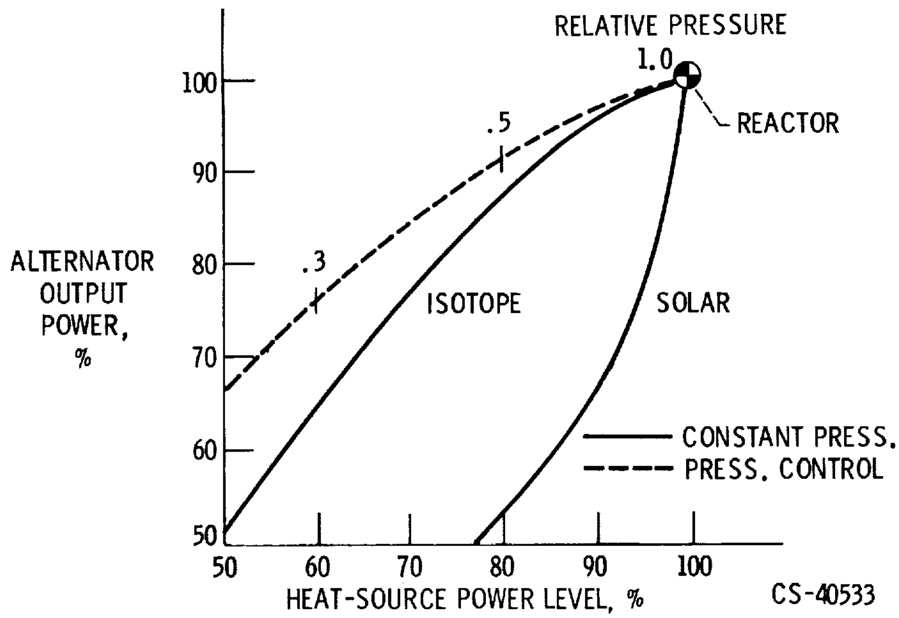

Figure V-53. - Pressure control effectiveness; two-shaft system.

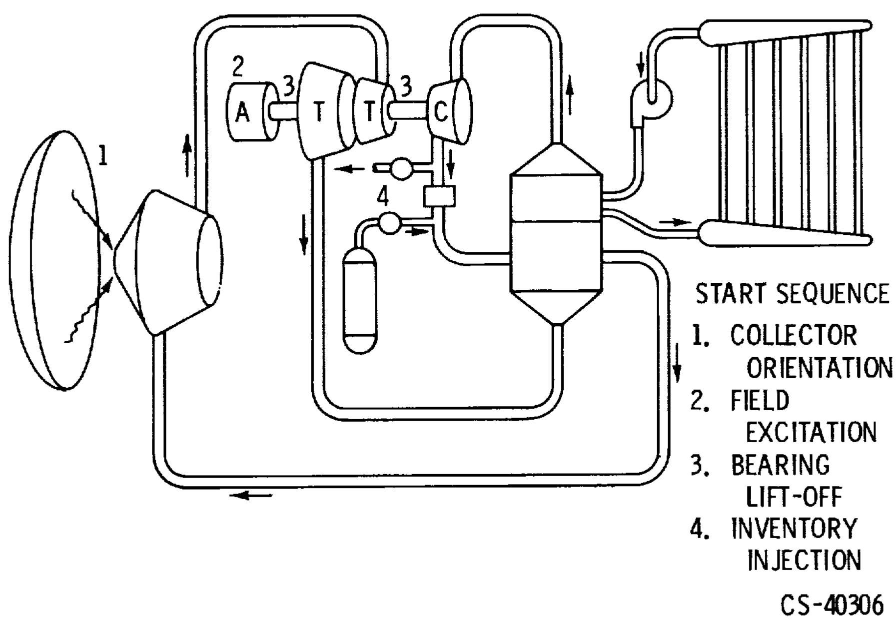

Figure V-54. - System configuration for start.

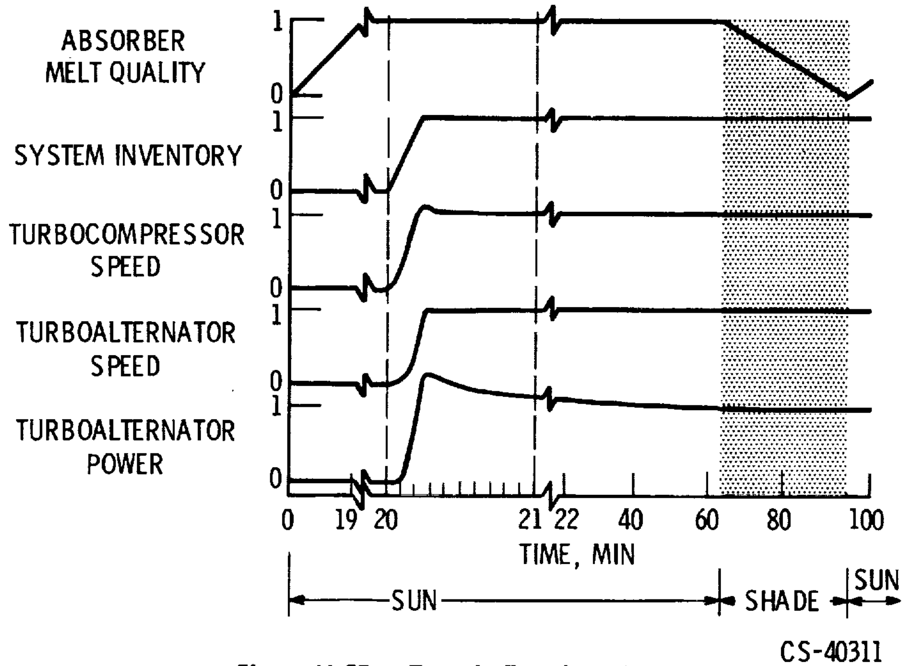

Figure V-55. - Two-shaft system start.

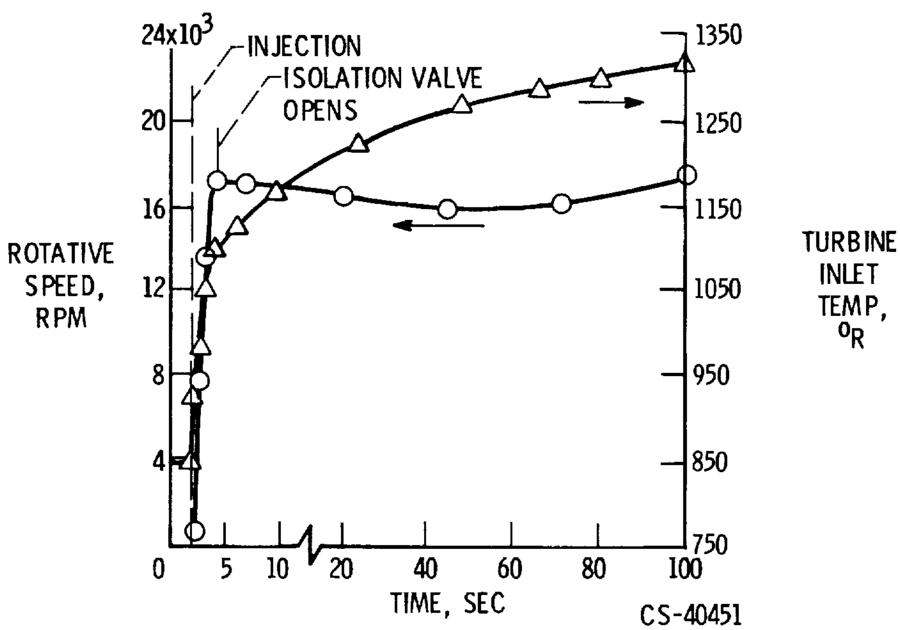

Figure V-56. - Turbocompressor experimental start.